MARTIN MARIETTA ENERGY SYSTEMS LIBRARIES

3 4456 0379855 8

ornl

ORNL/TM-12489

OAK RIDGE
NATIONAL
LABORATORY

MARTIN MARIETTA

Using Min-Max of Torque to Resolve Redundancy for a Mobile Manipulator

David B. Reister

OAK RIDGE NATIONAL LABORATORY
CENTRAL RESEARCH LIBRARY
CIRCULATION SECTION
4500N ROOM 175
LIBRARY LOAN COPY
DO NOT TRANSFER TO ANOTHER PERSON
If you wish someone else to see this report, send in name with report and the library will arrange a loan.

MANAGED BY
MARTIN MARIETTA ENERGY SYSTEMS, INC.
FOR THE UNITED STATES
DEPARTMENT OF ENERGY

This report has been reproduced directly from the best available copy.

Available to DOE and DOE contractors from the Office of Scientific and Technical Information, P.O. Box 62, Oak Ridge, TN 37831; prices available from (615) 576-8401, FTS 626-8401.

Available to the public from the National Technical Information Service, U.S. Department of Commerce, 5285 Port Royal Rd., Springfield, VA 22161.

This report was prepared as an account of work sponsored by an agency of the United States Government. Neither the United States Government nor any agency thereof, nor any of their employees, makes any warranty, express or implied, or assumes any legal liability or responsibility for the accuracy, completeness, or usefulness of any information, apparatus, product, or process disclosed, or represents that its use would not infringe privately owned rights. Reference herein to any specific commercial product, process, or service by trade name, trademark, manufacturer, or otherwise, does not necessarily constitute or imply its endorsement, recommendation, or favoring by the United States Government or any agency thereof. The views and opinions of authors expressed herein do not necessarily state or reflect those of the United States Government or any agency thereof.

ORNL/TM-12489

Engineering Physics and Mathematics Division

USING MIN-MAX OF TORQUE TO RESOLVE REDUNDANCY FOR A MOBILE MANIPULATOR

David B. Reister

DATE PUBLISHED — November 1993

Research sponsored by the
Engineering Research Program
Office of Basic Energy Sciences
U.S. Department of Energy

Prepared by the
OAK RIDGE NATIONAL LABORATORY
Oak Ridge, Tennessee 37831
managed by
MARTIN MARIETTA ENERGY SYSTEM, INC.
for the
U.S. DEPARTMENT OF ENERGY
under contract DE-AC05-84OR21400

MARTIN MARIETTA ENERGY SYSTEMS LIBRARIES

3 4456 0379855 8

CONTENTS

ABSTRACT ix

1. INTRODUCTION 1

2. NECESSARY CONDITIONS FOR THE MIN-MAX PROBLEM 5

3. MIN-MAX PATHS FOR A PLANAR MANIPULATOR 9

4. MIN-MAX PATHS FOR CESARm 27

5. CONCLUSIONS 61

REFERENCES 63

APPENDIX 65

LIST OF FIGURES

Figure		Page
1	Maximum torque (Q) versus height (z) for three subcases of case 1. The units of torque are newton meters and the units of height are meters	15
2	Maximum torque (Q) versus height (z) for four subcases of case 2. The units of torque are newton meters and the units of height are meters	16
3	Maximum torque (Q) versus height (z) for three subcases of case 3. The units of torque are newton meters and the units of height are meters	17
4	Maximum torque (Q) versus height (z) for two subcases of case 4. The units of torque are newton meters and the units of height are meters	18
5	Maximum torque (Q) versus height (z) for the nine subcases that satisfy the necessary conditions. The units of torque are newton meters and the units of height are meters	19
6	G^1 and G^2 versus the parameter k for case 3 ($G^2 = G^3$) and mode 1. The units of torque are newton meters	22
7	G^1 and G^2 versus the parameter k for case 3 ($G^2 = G^3$) and mode 3. The units of torque are newton meters	23
8	G^1 and G^2 versus the parameter k for case 4 ($G^2 = G^3$) and mode 0. The units of torque are newton meters	25
9	G^1 and G^2 versus the parameter k for case 4 ($G^2 = G^3$) and mode 2. The units of torque are newton meters	26
10	The seven degrees of freedom of the CESARm manipulator	28
11	Maximum torque (Q) versus height (z) for paths with three equal torques. The units of torque are newton meters and the units of height are meters	31
12	Maximum torque (Q) versus height (z) for three values of θ_4. The units of torque are newton meters and the units of height are meters	33
13	Maximum torque (Q) versus height (z) for the Long path and the Equal path. The units of torque are newton meters and the units of height are meters	35
14	Network diagram for the Bridge paths. Maximum torque (Q) versus height (z). The units of torque are newton meters and the units of height are meters	38
15	Network diagram for the Bridge paths. Maximum torque (Q) versus angle (θ_2). The units of torque are newton meters and the units of angle are degrees	39

LIST OF FIGURES (cont'd)

Figure		Page
16	Network diagram for the Bridge paths. Maximum torque (Q) versus angle (θ_3). The units of torque are newton meters and the units of angle are degrees	40
17	Maximum torque (Q) versus angle (θ_3) when $\theta_2 = 0$ and $\theta_4 = 45$. The units of torque are newton meters and the units of angle are degrees	41
18	Maximum torque (Q) versus angle (θ_3) when $\theta_2 = 38$ and $\theta_4 = 45$. The The units of torque are newton meters and the units of angle are degrees	43
19	Maximum torque (Q) versus angle (θ_3) when $\theta_2 = 83.6$ and $\theta_4 = 45$. The units of torque are newton meters and the units of angle are degrees	44
20	Maximum torque (Q) versus angle (θ_3) when $\theta_2 = 88.5$ and $\theta_4 = 45$. The units of torque are newton meters and the units of angle are degrees	45
21	Maximum torque (Q) versus angle (θ_3) when $\theta_2 = 91.5$ and $\theta_4 = 45$. The units of torque are newton meters and the units of angle are degrees	46
22	Maximum torque (Q) versus angle (θ_3) when $\theta_2 = 96.4$ and $\theta_4 = 45$. The units of torque are newton meters and the units of angle are degrees	47
23	Maximum torque (Q) versus angle (θ_3) when $\theta_2 = 116$ and $\theta_4 = 45$. The units of torque are newton meters and the units of angle are degrees	48
24	Maximum torque (Q) versus angle (θ_3) when $\theta_2 = 142$ and $\theta_4 = 45$. The units of torque are newton meters and the units of angle are degrees	49
25	Maximum torque (Q) versus angle (θ_3) when $\theta_2 = 180$ and $\theta_4 = 45$. The units of torque are newton meters and the units of angle are degrees	50
26	A closeup of the Equal bridge paths. Maximum torque (Q) versus height (z). The units of torque are newton meters and the units of height are meters	52
27	The Equal paths and their bridge paths. Maximum torque (Q) versus height (z). The units of torque are newton meters and the units of height are meters	53
28	A closeup of the Long bridge paths. Maximum torque (Q) versus height (z). The units of torque are newton meters and the units of height are meters	54
29	The Long paths and their bridge paths. Maximum torque (Q) versus height (z). The units of torque are newton meters and the units of height are meters	55

LIST OF TABLES

Table		Page
1	Definition of the four cases with equal torque at three joints for the planar manipulator	11
2	Definition of the 16 subcases for the planar manipulator	11
3	Evaluation of the necessary conditions for the 16 subcases	13
4	Definition of the six cases with equal torque at two joints for the planar manipulator	20
5	The 10 subcases defined in Table 2 that can reach the point z = 0.25	21
6	Four sets of joint angles that will reach each (Q,z) point	29
7	The joint angles at the significant points on the bridge paths	37
8	Evaluation of the necessary conditions for the lower branch of the Equal path	57
9	Evaluation of the necessary conditions for the Long path	57
10	Evaluation of the necessary conditions for the Bridge path from A to B	58
11	Evaluation of the necessary conditions for the Bridge path from A to C	58
12	Evaluation of the necessary conditions for the Bridge path from A to G	59
13	Evaluation of the necessary conditions for the Bridge path from B to E	59

ABSTRACT

We have considered the problem of determining the time trajectories of the joint variables of a mobile manipulator with many redundant degrees of freedom that will minimize the maximum value of the torque during a large scale motion by the manipulator. To create a well defined problem, we will divide the problem into two components: path planner and surveyor. The path planner will choose a path (between two points in Cartesian space) that will minimize the maximum value of the torque along the path. The input to the path planner is a network of path segments with the maximum value of the torque on each segment. The surveyor will find the points in joint space that are local minimums for the maximum value of the torque at each Cartesian position and define the network of path segments. In this paper, our focus will be on the surveyor and not on the path planner.

There is a large literature on algorithms for the solution of min-max problems. However, our min-max problem has an extra constraint on the joint variables. We seek a min-max at each Cartesian position rather than a global min-max. We have used the Kuhn-Tucker conditions to derive necessary conditions for the solution of our min-max problem. We find that the necessary conditions require that at one or more of the joints the magnitude of the normalized torques will be equal to the min-max value.

We have explored the torque surfaces for two mobile manipulators: a planar manipulator and the CESARm. The planar manipulator has three revolute joints. The paths with three equal torques cover the workspace and satisfy the necessary conditions.

The CESARm is a manipulator with three joint angles controlling the height of the arm. The paths with three equal torques have low values for the torque but they only cover part of the workspace and do not join together. Paths with two equal torques cover the workspace and bridge between the disjoint path segments. We have evaluated the necessary conditions for both the paths with three equal torques and the paths with two equal torques. In most cases, the paths satisfy the necessary conditions.

1. INTRODUCTION

Consider a mobile manipulator with many redundant degrees of freedom. A mission for the mobile manipulator robot will be subdivided into a sequence of tasks. During a task, the robot moves from an initial configuration to a final configuration while minimizing an objective function. The objective function could have several components including: obstacle avoidance, torque minimization, manipulability, and platform stability (see [1], [2], and [3]). In this paper, we consider a large scale motion while minimizing a single component of the objective function: the maximum value of the torque.

Manipulators consist of rigid links that are connected by joints. The joints can be revolute or prismatic. The number of degrees of freedom of a manipulator is the number of joint variables that must be specified to uniquely determine all of the parts of the machine. If the three vector P is the location of a point on the manipulator (usually the position of the end effector) in Cartesian space and θ is the vector of joint variables:

$$P = f(\theta) \tag{1}$$

For the manipulator, the Jacobian [J] maps the joint velocities to Cartesian velocities:

$$\dot{P} = J(\theta)\ \dot{\theta} \tag{2}$$

where

$$J(\theta) = \frac{\partial f(\theta)}{\partial \theta} \tag{3}$$

Furthermore, the transpose of the Jacobian maps the static Cartesian forces [F] from a load at the end of the manipulator to the static joint torques [τ] induced by the load:

$$\tau = J(\theta)^T F \tag{4}$$

Let Q be the maximum of the magnitudes of the joint torques (τ_i) divided by a limit for each joint (w_i):

$$Q(\theta) = \max_i |\tau_i| / w_i \tag{5}$$

Let Λ be the minimum value of $Q(\theta)$ at each Cartesian position:

$$\Lambda = \min_\theta Q(\theta) = \min_\theta \max_i |\tau_i| / w_i \tag{6}$$

Our objective is to determine paths for the joint variables (θ_i) that will minimize $Q(\theta)$ during the motion of the mobile manipulator from an initial position (P^i) to a final position (P^f). Solving this min-max problem will resolve the redundancy for the joint variables.

In classical optimization theory, the methods that are used to minimize a function at a point are different than the methods that are used to minimize a functional on a trajectory from an initial position to a final position. At an unconstrained interior minimum of a function of one variable, the derivative is equal to zero. For the most simple problem in the calculus of variations, the objective is to find a function [x(t)] such that $x(t_i) = a$, $x(t_f) = b$, and the functional [Φ] is a minimum, where:

$$\Phi = \int_{t_i}^{t_f} U(x(t),\dot{x}(t),t)\, dt \tag{7}$$

At every point on the trajectory, the variables must satisfy the Euler-Lagrange equation:

$$\frac{d}{dt}\frac{\partial U}{\partial \dot{x}} - \frac{\partial U}{\partial x} = 0 \tag{8}$$

Only in the special case where the function U does not depend on $\dot{x}$ will the Euler-Lagrange equation require that the function U be at its minimum for all points on the path from a to b.

We have not found any papers on min-max problems over a trajectory. However, if there were a few isolated points on the trajectory with maximum torque, there would be no need to minimize the torque at the other points. Thus, the min-max criterion may not constrain or determine most points on the path and the path may not be unique. For example, suppose that you wanted to plan a path that would minimize the maximum elevation during an automobile trip from Saint Louis, Missouri to Salt Lake City, Utah.

The maximum elevation would probably be in the Rocky Mountain states. Thus, the criterion to minimize the maximum elevation during the trip would not give you any guidance as you traveled across the Great Plains states.

To create a well defined problem, we will divide the problem into two components: path planner and surveyor. The path planner that will choose a path between two points in Cartesian space that will minimize the maximum value of the torque along the path. The input to the path planner is a network of path segments with the maximum value of the torque on each segment. The surveyor will explore the joint space and define the network of path segments. In this paper, our focus is on the surveyor and not on the path planner.

Given a Cartesian position (P), we can solve the min-max problem. Conventional search techniques slowly solve min-max problems. The basic reason is that the conventional search techniques assume that the function is differentiable and $Q(\theta)$ is usually not differentiable at the minimum. Many algorithms that solve min-max problems have been developed (see Polak [4]).

In the next section, we will convert the min-max problem into a nonlinear programming problem and use the Kuhn-Tucker conditions to derive necessary conditions for the solution of the min-max problem. We shall find that the necessary conditions require that at one or more of the joints the magnitude of the normalized torques will be equal to the min-max value. However, an isolated minimum may not be useful for a large scale motion.

In the subsequent sections, we will explore continuous paths for the joint variables that will minimize the maximum of the normalized torques during a large scale motion by the mobile manipulator. In the third section, we will find min-max paths for a planar manipulator. In the fourth section, we will explore min-max paths for the CESARm. The final section will present our conclusions.

2. NECESSARY CONDITIONS FOR THE MIN-MAX PROBLEM

There is a large literature on algorithms for the solution of min-max problems. An example is a recent paper by Polak [4]. However, our min-max problem has an extra constraint on the joint variables [Eq. (1)]. Consequently, the necessary conditions for our min-max problem are more general than for the standard problem. Polak calls a point that satisfies the necessary conditions for the standard problem a Danskin point. Our conditions will reduce to the conditions for the Danskin point when the extra constraint is removed.

We will convert our min-max problem into a nonlinear programming problem and use the Kuhn-Tucker conditions to derive necessary conditions for the solution of the min-max problem. To simplify our notation, we will define the functions $G^i(\theta)$ by:

$$G^i(\theta) = |\tau_i| / w_i \tag{9}$$

Following Polak, we convert Eq. (6) from an unconstrained nondifferentiable optimization problem to a constrained differentiable optimization problem:

Find θ to minimize Λ subject to:

$$\Lambda \geq G^i(\theta) \tag{10}$$

We introduce the nonnegative slack variables (σ_i):

$$\sigma_i = \Lambda - G^i(\theta) \geq 0 \tag{11}$$

We assume that the position of the end effector is fixed:

$$f(\theta) = P^* \tag{12}$$

where P^* is a constant. Define the Lagrangian (L) by:

$$L = -\Lambda + \sum_k \lambda_k (f_k(\theta) - P_k^*) + \sum_i \mu_i (\Lambda - G^i(\theta) - \sigma_i) \tag{13}$$

The Lagrangian depends on five variables (Λ, θ, λ, μ, σ). The first four variables are unrestricted in sign while the last variable (σ) is nonnegative. The first order necessary conditions for the unrestricted variables require that all first order partial derivatives of L with respect to the unrestricted variables must vanish. The Kuhn-Tucker conditions provide the first order necessary conditions for the restricted variables. The first order necessary conditions are:

$$\sum_i \mu_i = 1 \tag{14}$$

$$\sum_i \mu_i \frac{\partial G^i(\theta^*)}{\partial \theta_j} = \sum_k \lambda_k \frac{\partial f_k(\theta^*)}{\partial \theta_j} \tag{15}$$

$$\mu_i \geq 0 \tag{16}$$

$$\sum_i \mu_i \sigma_i(\theta^*) = 0 \tag{17}$$

We can use the first order necessary conditions to demonstrate that at the min-max point (θ^*) the magnitude of the normalized torques will be equal to the min-max value (Λ) at one or more of the joints. Since both μ and σ are nonnegative, every term on the left side of Eq. (17) must be zero:

$$\mu_i \, \sigma_i = 0 \tag{18}$$

Thus, whenever μ_i is positive, the corresponding slack variable (σ_i) will be zero. At each point where the slack variable is zero, the normalized torque (G^i) is equal to the min-max value (Λ). Equation (14) requires that at least one of the μ_i must be positive.

We can classify the sets of points that satisfy the necessary conditions based on the number of the μ_i that are positive. For Class 1, one of the μ_i will be positive. For Class 2, two of the μ_i will be positive. For Class n, n of the μ_i will be positive. For Class 1, one of the $G^i(\theta)$ is larger than the others ($Q(\theta) = G^k(\theta)$) and the necessary conditions simplify to the familiar conditions of classical optimization. If we let $\lambda = 0$, Eq. (15) becomes:

$$\frac{\partial G^k(\theta)}{\partial \theta_j} = 0 \tag{19}$$

We can think of the $G^i(\theta)$ as surfaces in parameter space. For Class 2, two of the surfaces intersect at the min-max point (θ^*):

$$\Lambda = Q(\theta^*) = G^k(\theta^*) = G^m(\theta^*) \tag{20}$$

Near the min-max point, there will be a region (A) where $Q(\theta) = G^k(\theta)$ and a region (B) where $Q(\theta) = G^m(\theta)$. If we ignore the end effector constraint (let $\lambda = 0$) and move from region A through the min-max point to region B, $Q(\theta)$ will decrease as we approach θ^* and increase as we move away from θ^*. Normally, $Q(\theta)$ is not differentiable at the min-max point. When $\lambda = 0$, Eq. (15) is a generalization of classical optimization condition:

$$\sum_i \mu_i \frac{\partial G^i(\theta^*)}{\partial \theta_j} = 0 \tag{21}$$

For the classical optimization condition [Eq. (19)], all of the partial derivatives of $Q(\theta)$ are equal to zero. For the generalized condition [Eq. (21)], all of the partial derivatives of a weighted average of the $G^i(\theta)$ are equal to zero.

For Class n, n of the surfaces intersect at the min-max point. We will solve the min-max problem by identifying all of the points in all of the classes. For Class 1, we will find all of the points that satisfy the classical optimization condition [Eq.(19)]. For the other classes, we will identify all of the points that are on the intersections of two or more surfaces and test whether or not the necessary conditions are satisfied.

To find the global min-max, we plot $Q(\theta)$ vs $P(\theta)$ for all of the points in all of the classes that satisfy the necessary conditions. The global min-max at the point $P(\theta)$ has the lowest value for $Q(\theta)$.

The surveyor will identify all of the type A paths (paths with continuous joint variables that link points in the work space and satisfy the necessary conditions). If there are points in the workspace that cannot be linked by type A paths, the surveyor will identify type B paths to bridge between the type A paths. The type B paths have continuous joint variables, are members of one of the classes, link points in the work space, and may not satisfy the necessary conditions.

Equation (15) is our generalization of the conditions for a Danskin point. If we ignore the constraint [Eq. (12)], $\lambda = 0$ and Eq. (15) reduces to Polak's condition [his Eq. (7)]. It is useful to express Eq. (15) in matrix notation. Define the elements of the matrix A by:

$$a_{ij} = \frac{\partial G^i(\theta)}{\partial \theta_j} \tag{22}$$

Then Eq. (15) may be written:

$$A^T \mu = J^T \lambda \tag{23}$$

In Polak's unconstrained case, $\lambda = 0$ and A must be singular. In our constrained case, A can be singular or nonsingular.

We have demonstrated that the magnitude of the normalized torques will be equal to the min-max value at one or more of the joints. In the examples that we will consider in this paper, the best Class 3 and Class 2 paths will have lower values for the normalized torques than any of the Class 1 paths. However, we can create a simple example where the Class 1 paths are best. Consider a manipulator with stacked prismatic joints. The z coordinate of the arm's tip (P) is given by:

$$z = z_0 + \sum_i q_i \theta_i \tag{24}$$

For this example, the components of J are constants ($J_i = q_i$) and the components of G are constants ($G^i = g_i$). Thus, the elements of the matrix A are zero ($a_{ij} = 0$). Assume that the first component of G is the largest ($g_1 > g_i$ for $i > 1$). Then, $Q = g_1$, $\mu_1 = 1$, $\mu_i = 0$ for $i > 1$, $\sigma_1 = 0$, and $\sigma_i > 0$ for $i > 1$.

3. MIN-MAX PATHS FOR A PLANAR MANIPULATOR

We consider a mobile planar manipulator with three revolute joints (θ_i). The platform can move in the x direction. The manipulator can reach points in the (x,z) plane. We assume that the platform will control the x coordinate of the arm's tip (P) [we recognize that obstacles could prevent free motion of the platform in the x direction]. If the lengths of the three links of the arm are (1, 1, and 0.5) meters, the z coordinate of P is given by:

$$z = \sin \psi_1 + \sin \psi_2 + 0.5 \sin \psi_3 \tag{25}$$

where: $\psi_1 = \theta_1$, $\psi_2 = \theta_1 + \theta_2$, and $\psi_3 = \theta_1 + \theta_2 + \theta_3$. The components of the Jacobian are:

$$J_1 = \cos \psi_1 + \cos \psi_2 + 0.5 \cos \psi_3 \tag{26}$$

$$J_2 = \cos \psi_2 + 0.5 \cos \psi_3 \tag{27}$$

$$J_3 = 0.5 \cos \psi_3 \tag{28}$$

If the force is directed downward ($F_z = -1$ newton), the joint torques are given by:

$$\tau_i = - J_i \tag{29}$$

We will assume that the weights for each joint are equal: $w_i = 1$.

We have three joint angles controlling the height of the arm (z). Given a desired change in height, we would like to determine paths for the joint angles that minimize the maximum of the torque during the motion. In the last section, we demonstrated that at the min-max point the magnitude of the torques will be equal to the min-max value at one or more of the joints. We begin by exploring the Class 3 paths where the magnitudes of all three torques are equal during the motion (subsequently, we will consider the Class 2 paths where two of the three torques are equal and the Class 1 paths). We distinguish four cases in Table 1.

For each of the four cases, we can solve Eqs. (26) to (28) and determine two conditions on the link angles (ψ). For example when $\tau_1 = \tau_2 = \tau_3$, $J_1 = J_2 = J_3$ and subtracting Eq. (27) from Eq. (26) yields the first condition for the first case ($\cos \psi_1 = 0$).

Each of the two conditions has two solutions. For the condition $\cos \psi_1 = 0$, the two solutions are: $\psi_1 = \pm \pi / 2$. For the condition $\cos \psi_1 + \cos \psi_2 = 0$, the two solutions are: $\psi_2 = \pi \pm \psi_1$. Thus, each case has four subcases. We define the 16 subcases for the planar manipulator in Table 2.

For each of the 16 subcases, we have defined the three link angles in terms of a single parameter (ϕ). The last column in Table 2 expresses z as a function of ϕ. By relating the three link angles to ϕ, we have resolved the redundancy. Thus, Table 2 displays 16 ways to resolve the redundancy.

We will assume that z can have both positive and negative values (if z cannot have negative values, we could raise the base of the manipulator by 2.5 meters). All of the expressions for z have the form: $z = a + b \sin \phi$. In some subcases, $a = 0$ and z will range from -b to b as ϕ ranges from $-\pi / 2$ to $\pi / 2$. In the subcases where a is not equal to zero, there is another subcase where $a_1 = -a_2$ and $b_1 = b_2$ (for example, subcases 1.2 and 1.4 and subcases 2.2 and 2.3). Thus, all of the subcases exhibit symmetry between positive and negative values of z.

Next, we will determine which of the 16 subcases satisfy the necessary conditions [Eqs.(14), (15) and (16)]. We begin by determining the elements of the A matrix [see Eq. (22)]. For the planar manipulator, the functions $G^i(\theta)$ are given by:

$$G^i(\theta) = d_i J_i \tag{30}$$

where the constants $d_i = \pm 1$ and the signs are chosen to make the $G^i(\theta)$ nonnegative. We define the functions $S_i(\theta)$ by:

$$S_1(\theta) = \sin \psi_1 + \sin \psi_2 + 0.5 \sin \psi_3 \tag{31}$$

$$S_2(\theta) = \sin \psi_2 + 0.5 \sin \psi_3 \tag{32}$$

$$S_3(\theta) = 0.5 \sin \psi_3 \tag{33}$$

Table 1. Definition of the four cases with equal torque at three joints for the planar manipulator.

Case	Torque Signs	First Condition	Second Condition
1	$\tau_1 = \tau_2 = \tau_3$	$\cos \psi_1 = 0$	$\cos \psi_2 = 0$
2	$\tau_1 = \tau_2 = -\tau_3$	$\cos \psi_1 = 0$	$\cos \psi_2 + \cos \psi_3 = 0$
3	$\tau_1 = -\tau_2 = \tau_3$	$\cos \psi_1 + \cos \psi_2 = 0$	$\cos \psi_2 + \cos \psi_3 = 0$
4	$\tau_1 = -\tau_2 = -\tau_3$	$\cos \psi_2 = 0$	$\cos \psi_1 + \cos \psi_3 = 0$

Table 2. Definition of the 16 subcases for the planar manipulator.

Subcase	ψ_1	ψ_2	ψ_3	$z = f(\phi)$
1.1	$\pi/2$	$-\pi/2$	ϕ	$\frac{1}{2} \sin \phi$
1.2	$\pi/2$	$\pi/2$	ϕ	$2 + \frac{1}{2} \sin \phi$
1.3	$-\pi/2$	$\pi/2$	ϕ	$\frac{1}{2} \sin \phi$
1.4	$-\pi/2$	$-\pi/2$	ϕ	$-2 + \frac{1}{2} \sin \phi$
2.1	$\pi/2$	$\pi + \phi$	ϕ	$1 - \frac{1}{2} \sin \phi$
2.2	$\pi/2$	$\pi - \phi$	ϕ	$1 + \frac{3}{2} \sin \phi$
2.3	$-\pi/2$	$\pi - \phi$	ϕ	$-1 + \frac{3}{2} \sin \phi$
2.4	$-\pi/2$	$\pi + \phi$	ϕ	$-1 - \frac{1}{2} \sin \phi$
3.1	ϕ	$\pi + \phi$	ϕ	$\frac{1}{2} \sin \phi$
3.2	ϕ	$\pi - \phi$	ϕ	$\frac{5}{2} \sin \phi$
3.3	ϕ	$\pi - \phi$	$-\phi$	$\frac{3}{2} \sin \phi$
3.4	ϕ	$\pi + \phi$	$-\phi$	$-\frac{1}{2} \sin \phi$
4.1	$\pi - \phi$	$-\pi/2$	ϕ	$-1 + \frac{3}{2} \sin \phi$
4.2	$\pi - \phi$	$\pi/2$	ϕ	$1 + \frac{3}{2} \sin \phi$
4.3	$\pi + \phi$	$\pi/2$	ϕ	$1 - \frac{1}{2} \sin \phi$
4.4	$\pi + \phi$	$-\pi/2$	ϕ	$-1 - \frac{1}{2} \sin \phi$

Using the S_i, the A matrix is:

$$A^T = -\begin{bmatrix} d_1 S_1 & d_2 S_2 & d_3 S_3 \\ d_1 S_2 & d_2 S_2 & d_3 S_3 \\ d_1 S_3 & d_2 S_3 & d_3 S_3 \end{bmatrix} \tag{34}$$

Our goal is to find the μ_i that satisfy Eq. (23). We will first solve for an intermediate vector (η):

$$\eta_i = -\mu_i / \lambda \tag{35}$$

Using the η_i, Eq. (23) is:

$$d_1 S_1 \eta_1 + d_2 S_2 \eta_2 + d_3 S_3 \eta_3 = J_1 \tag{36}$$

$$d_1 S_2 \eta_1 + d_2 S_2 \eta_2 + d_3 S_3 \eta_3 = J_2 \tag{37}$$

$$d_1 S_3 \eta_1 + d_2 S_3 \eta_2 + d_3 S_3 \eta_3 = J_3 \tag{38}$$

Subtracting Eq. (37) from Eq. (36) and subtracting Eq. (38) from Eq. (37), Eqs. (36) to (38) may be written in triangular form:

$$d_1 \eta_1 = \text{ctn}\ \psi_1 \tag{39}$$

$$d_1 \eta_1 + d_2 \eta_2 = \text{ctn}\ \psi_2 \tag{40}$$

$$d_1 \eta_1 + d_2 \eta_2 + d_3 \eta_3 = \text{ctn}\ \psi_3 \tag{41}$$

The constants $d_i = \pm 1$ and their signs are chosen to make the $G^i(\theta)$ nonnegative. Expressions for the three link angles (ψ_i) are given in Table 2 (as functions of the parameter ϕ). Given values for the d_i and the ψ_i, Eqs. (39) to (41) can be solved for the η_i. The values of d_i and η_i are displayed in Table 3 for the 16 subcases.

Our goal is to find the μ_i that satisfy the first order necessary conditions [Eqs. (14) to (16)]. We have introduced the intermediate vector (η) and solved Eq. (15) to find the values of η_i displayed in Table 3. We can choose the normalization factor (λ) to insure that Eq. (14) is satisfied:

$$\lambda = -1 / \sum_i \eta_i \tag{42}$$

$$\mu_i = -\lambda * \eta_i \tag{43}$$

The remaining condition is that the μ_i must not be negative [Eq. (16)]. The corresponding condition on the η_i is that they must all have the same sign. In 13 of the 16 subcases in Table 3, the η_i have the same signs. Thus, the μ_i satisfy the necessary conditions for 13 of the 16 subcases.

Table 3. Evaluation of the necessary conditions for the 16 subcases.

Subcase	d_1	d_2	d_3	η_1	η_2	η_3	Satisfy?
1.1	+ 1	+ 1	+ 1	0	0	ctn ϕ	Yes
1.2	+ 1	+ 1	+ 1	0	0	ctn ϕ	Yes
1.3	+ 1	+ 1	+ 1	0	0	ctn ϕ	Yes
1.4	+ 1	+ 1	+ 1	0	0	ctn ϕ	Yes
2.1	- 1	- 1	+ 1	0	- ctn ϕ	0	Yes
2.2	- 1	- 1	+ 1	0	ctn ϕ	2 ctn ϕ	Yes
2.3	- 1	- 1	+ 1	0	ctn ϕ	2 ctn ϕ	Yes
2.4	- 1	- 1	+ 1	0	- ctn ϕ	0	Yes
3.1	+ 1	- 1	+ 1	ctn ϕ	0	0	Yes
3.2	+ 1	- 1	+ 1	ctn ϕ	2 ctn ϕ	2 ctn ϕ	Yes
3.3	+ 1	- 1	+ 1	ctn ϕ	2 ctn ϕ	0	Yes
3.4	+ 1	- 1	+ 1	ctn ϕ	0	- 2 ctn ϕ	No
4.1	- 1	+ 1	+ 1	ctn ϕ	ctn ϕ	ctn ϕ	Yes
4.2	- 1	+ 1	+ 1	ctn ϕ	ctn ϕ	ctn ϕ	Yes
4.3	- 1	+ 1	+ 1	- ctn ϕ	- ctn ϕ	ctn ϕ	No
4.4	- 1	+ 1	+ 1	- ctn ϕ	- ctn ϕ	ctn ϕ	No

We will examine plots of maximum torque (Q) versus height (z) for the four cases. We will not consider the three subcases that do not satisfy the necessary contions. Furthermore, subcase 1.3 will not be considered bacause it is so similar to subcase 1.1 (in 1.1 the first joint is up, while in 1.3 the first joint is down).

The three subcases of case 1 are displayed in Fig. 1. All three subcases have the same range (one meter). For each subcase, the torque increases from zero to a maximum and the decreases to zero as the manipulator moves through its range. Each subcase has a different value of z at its midpoint (0.0 for subcase 1.1, 2.0 for subcase 1.2, and -2.0 for subcase 1.4).

The four subcases of case 2 are displayed in Fig. 2. Two of the subcases have a one meter range while the other two have a three meter range. For each subcase, the torque increases from zero to a maximum and then decreases to zero as the manipulator moves through its range (the maximum values for the torque for all 13 subcases are identical). For two of the subcases, the midpoint of the range is 1.0 and for the other two the midpoint is -1.0. If we added subcases 2.1 and 2.4 to Fig. 1, we would find that the new subcases fill the gaps in Fig. 1 and we would have five disjoint options for covering the total five meter range. Subcases 2.2 and 2.3 cover the same five meter range and overlap near 0.0.

The three subcases of case 3 are displayed in Fig. 3. Each of the subcases has a different range (one, three, and five meters). The midpoint of the range is 0.0 for all three subcases. Subcase 3.1 covers the same range as Subcase 1.1. The two subcases of case 4 are displayed in Fig. 4. The two subcases have the same workspace as subcases 2.2 and 2.3.

We have found three groups of subcases {(1.1, 1.3, 3.1), (2.2, 4.2), (2.3, 4.1)}that have identical values for Q in identical workspaces. However, the values of the link angles are not identical within these groups. If we were considering the more general problem of avoiding obstacles while minimizing the maximum torque, one member of the group might be better than the others.

We began with 13 subcases that satisfied the necessary conditions. We have found five configurations with a one meter workspace, three configurations with a three meter workspace, and one configuration with a five meter workspace. Which of the options (summarized in Fig. 5) should we use to move from an initial value of z to a final value?

All but one of the options (subcase 1.1) has a portion of the workspace where it is superior to any of the other options. For example, subcase 3.2 is best near the upper and lower limits of the workspace. Subcase 1.2 is best for a small interval beyond z = 1.5 meters. Subcases 2.2 and 2.3 are better than subcase 1.1 on the middle interval [-0.5, 0.5].

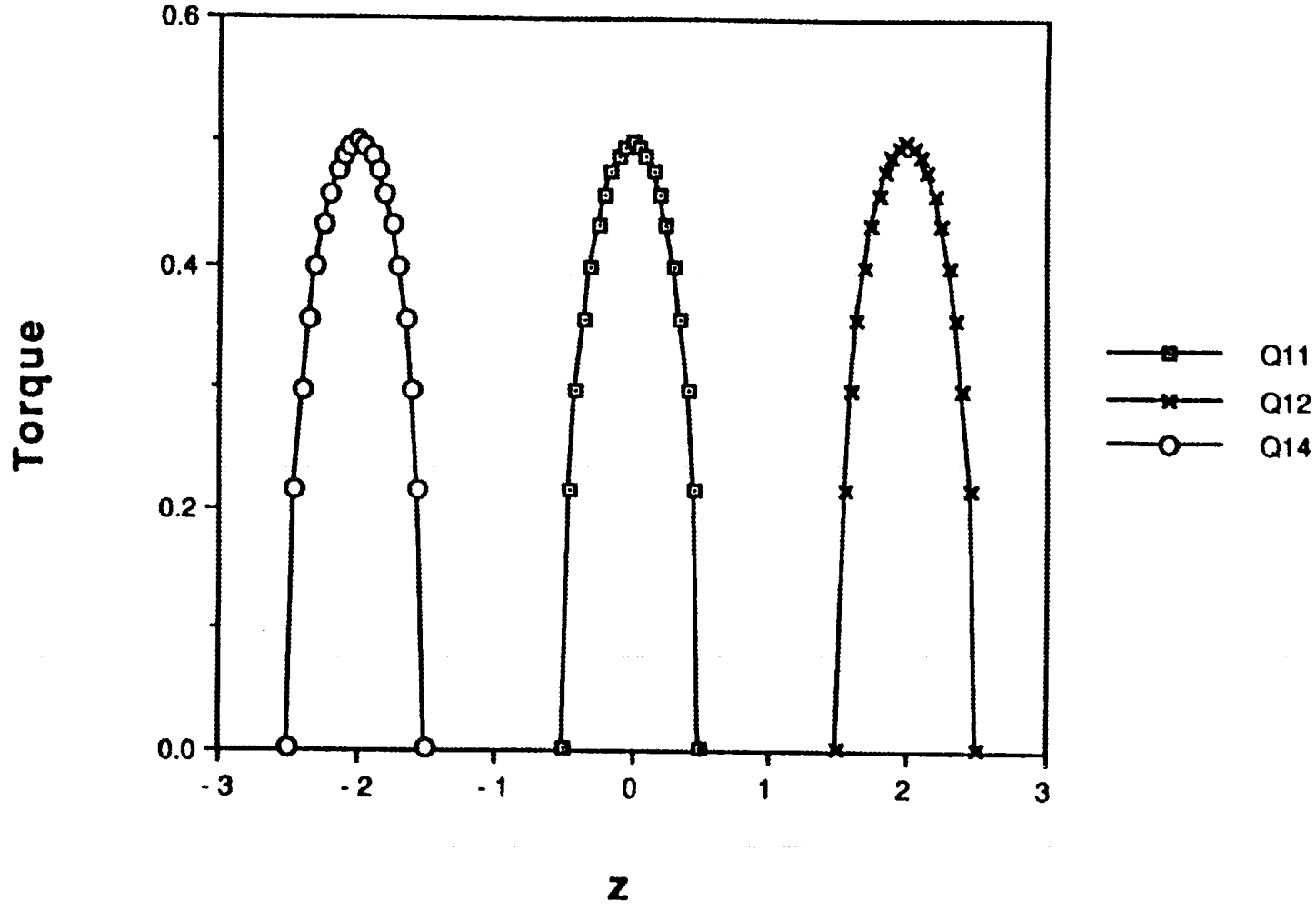

Fig. 1. Maximum torque (Q) versus height (z) for three subcases of case 1. The units of torque are newton meters and the units of height are meters.

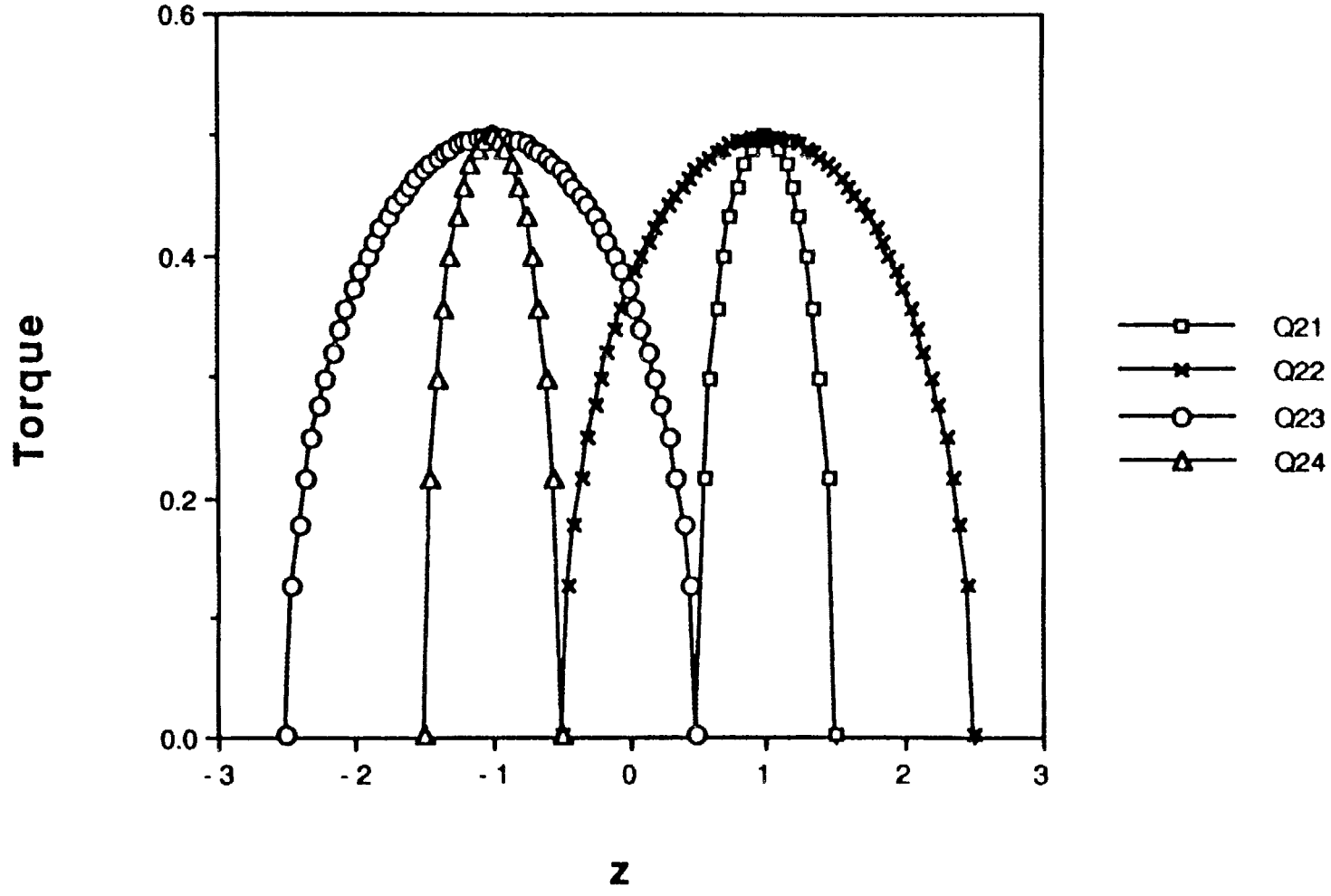

Fig. 2. Maximum torque (Q) versus height (z) for four subcases of case 2. The units of torque are newton meters and the units of height are meters.

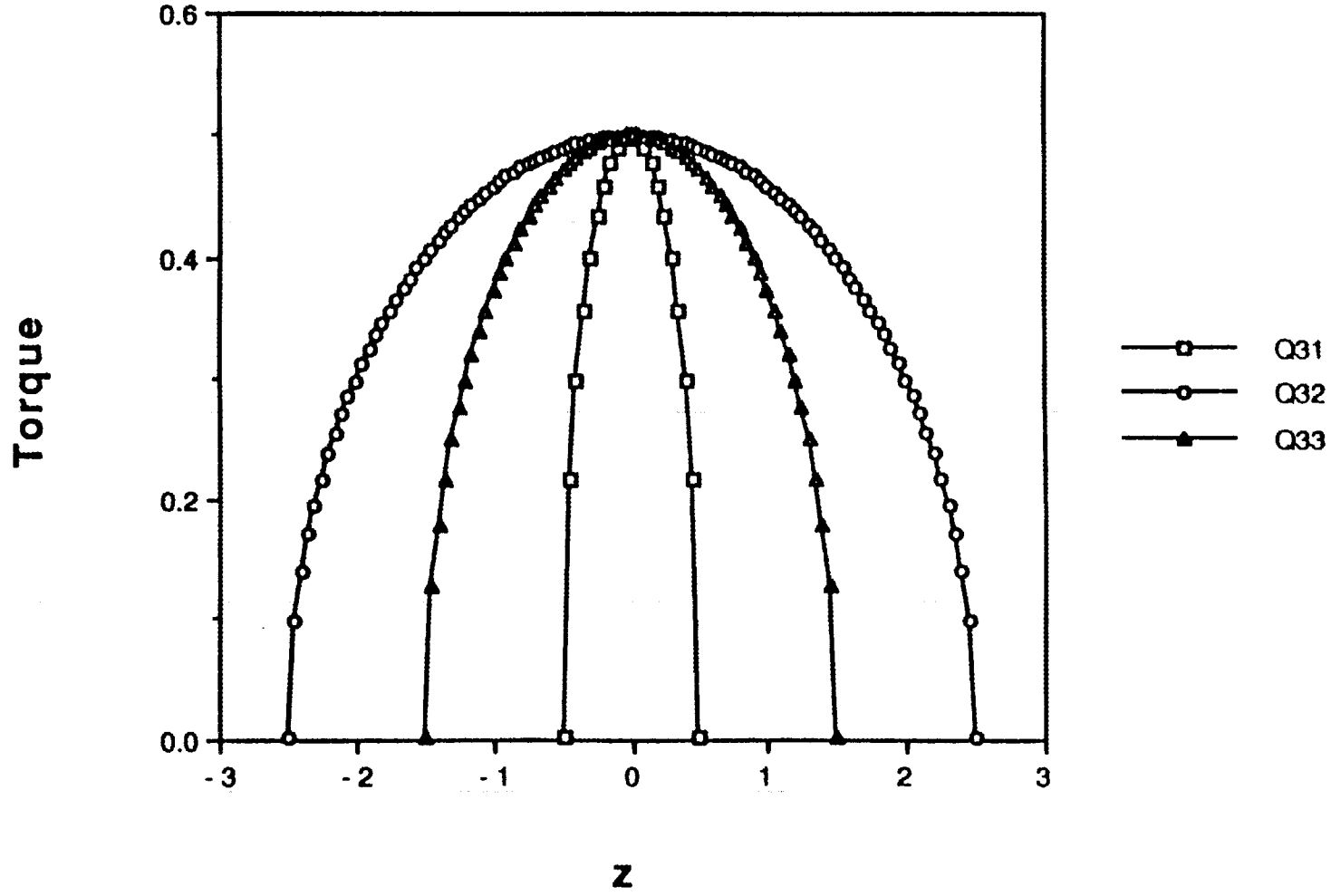

Fig. 3. Maximum torque (Q) versus height (z) for three subcases of case 3. The units of torque are newton meters and the units of height are meters.

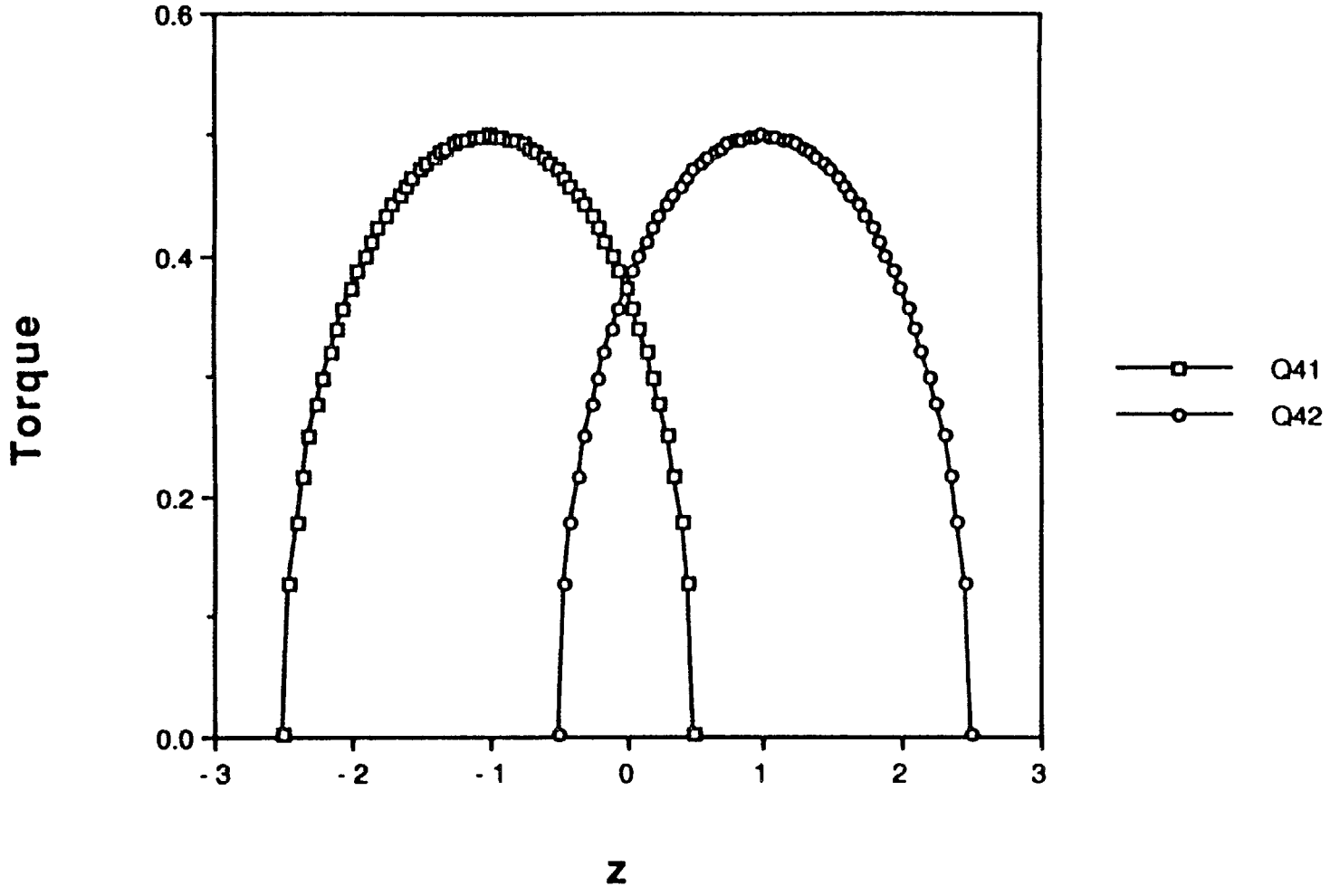

Fig. 4. Maximum torque (Q) versus height (z) for two subcases of case 4. The units of torque are newton meters and the units of height are meters.

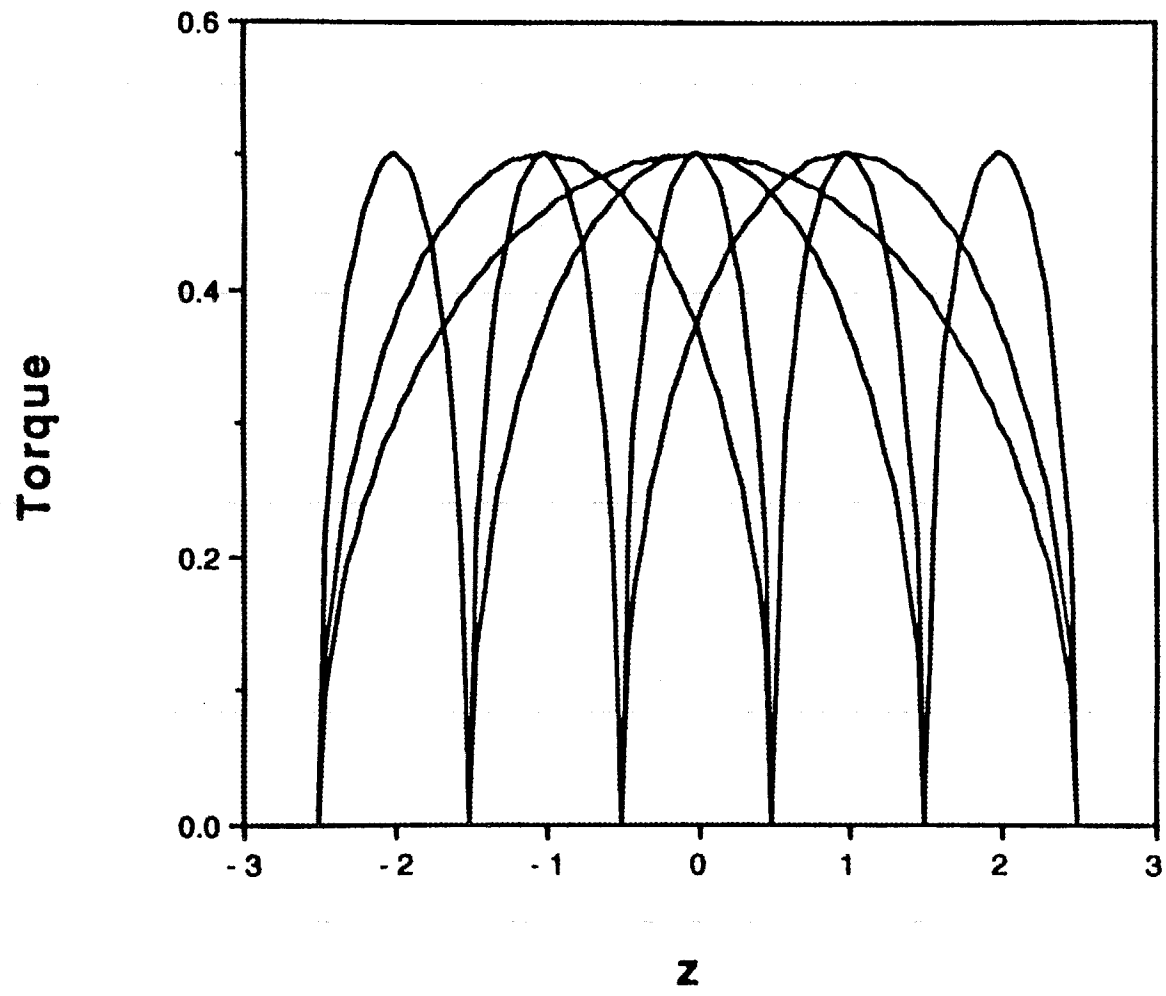

Fig. 5. Maximum torque (Q) versus height (z) for the nine subcases that satisfy the necessary conditions. The units of torque are newton meters and the units of height are meters.

A path planner for the manipulator could choose the option that was best for each task. If the planner wanted to choose a single option that was occasionally best and always close to the torque minimum, it could choose subcase 3.2.

We conclude this section by considering Class 2 paths that have equal torque magnitudes at two of the three joints and the Class 1 paths. We distinguish six cases in Table 4. When the torques are equal at two of the joints, we can derive one constraint on the link angles (ψ_i) and could express the three link angles in terms of two parameters. However, we will assume that z is constant and express the three link angles in terms of one parameter.

Table 4. Definition of the six cases with equal torque at two joints for the planar manipulator.

Case	Torque Signs	Condition	Solution
1	$\tau_1 = \tau_2$	$\cos \psi_1 = 0$	$\psi_1 = \pm \pi / 2$
2	$\tau_1 = - \tau_2$	$\cos \psi_1 + 2 \cos \psi_2 + \cos \psi_3 = 0$	
3	$\tau_2 = \tau_3$	$\cos \psi_2 = 0$	$\psi_2 = \pm \pi / 2$
4	$\tau_2 = - \tau_3$	$\cos \psi_2 + \cos \psi_3 = 0$	$\psi_3 = \pi \pm \psi_2$
5	$\tau_1 = \tau_3$	$\cos \psi_1 + \cos \psi_2 = 0$	$\psi_2 = \pi \pm \psi_1$
6	$\tau_1 = - \tau_3$	$\cos \psi_1 + \cos \psi_2 + \cos \psi_3 = 0$	

In Table 4, we defined six cases with equal torque magnitudes at two joints, while we defined four cases with equal torque magnitudes at three joints in Table 1. As we consider all cases that have equal torques at two joints, we will find isolated points in the three dimensional space of link angles where the torques are equal at three joints. Thus, as we consider all of the points in link space that are in Case 1 in Table 4, we will find isolated points that are in Cases 1 and 2 in Table 1. Similarly, Cases 3 and 4 in Table 1 are examples of Case 2 in Table 4. To examine all of the cases in Table 1, we need to consider Cases 1 and 2 in Table 4, or Cases 3 and 4, or Cases 5 and 6. Since we have a simple analytical expression for the conditions on the link angles in Cases 3 and 4, we will focus on Cases 3 and 4.

We will assume that z = 0.25. This point is in the workspace of 10 of the 16 Subcases listed in Table 2 (see Table 5). As the parameter k increases from 0 to 100, the link angle ψ_3 will increase from $- \pi / 2$ to $\pi / 2$. For Cases 3 and 4, the condition in Table

4 will provide two solutions for ψ_2 when ψ_3 is known. Given ψ_3, ψ_2, and z, Eq. (25) may yield two solutions for ψ_1. Thus, for each value of the parameter k, we can determine up to four solutions for the link angles. We will use a mode variable with a range from 0 to 3 to identify the four solutions.

Table 5. The 10 subcases defined in Table 2 that can reach the point z = 0.25.

Subcase	ψ_1	ψ_2	ψ_3	k	Figure
1.1	$\pi / 2$	$-\pi / 2$	ϕ	66	7
1.3	$-\pi / 2$	$\pi / 2$	ϕ	67	6
2.2	$\pi / 2$	$\pi - \phi$	ϕ	33	9
2.3	$-\pi / 2$	$\pi - \phi$	ϕ	82	9
3.1	ϕ	$\pi + \phi$	ϕ	67	8
3.2	ϕ	$\pi - \phi$	ϕ	53	9
3.3	ϕ	$\pi - \phi$	$-\phi$	45	8
3.4	ϕ	$\pi + \phi$	$-\phi$	67	9
4.1	$\pi - \phi$	$-\pi / 2$	ϕ	81	7
4.2	$\pi - \phi$	$\pi / 2$	ϕ	33	6

In Case 3, $\tau_2 = \tau_3$. Thus, $G^2 = G^3$. G^1 and G^2 are plotted in Fig. 6 as a function of the parameter k for Case 3 and mode 1. Λ is the minimum value of the maximum of the G^i. In Fig. 6, there are two local minima at k = 33 and k = 67. At each local minima, $G^1 = G^2 = G^3$. Hence, there are no local minima at which only two of the joint torques are equal. At each local minima, we can determine the link angles and identify which of the 16 subcases in Table 2 has occurred. At k = 33, the subcase is 4.2 and the subcase is 1.3 when k = 67. We will identify the value of k and the figure number for each of the ten subcases in Table 5.

G^1 and G^2 are plotted in Fig. 7 for Case 3 and mode 3. In Fig. 7, there is one local minima at k = 81 and a point where $G^1 = G^2$ that is not a local minima at k = 66. At k = 66, the subcase is 1.1 and the subcase is 4.1 when k = 81. Although subcase 1.1 satisfies the necessary conditions, we previously noted that it was never the best option for any region of the workspace.

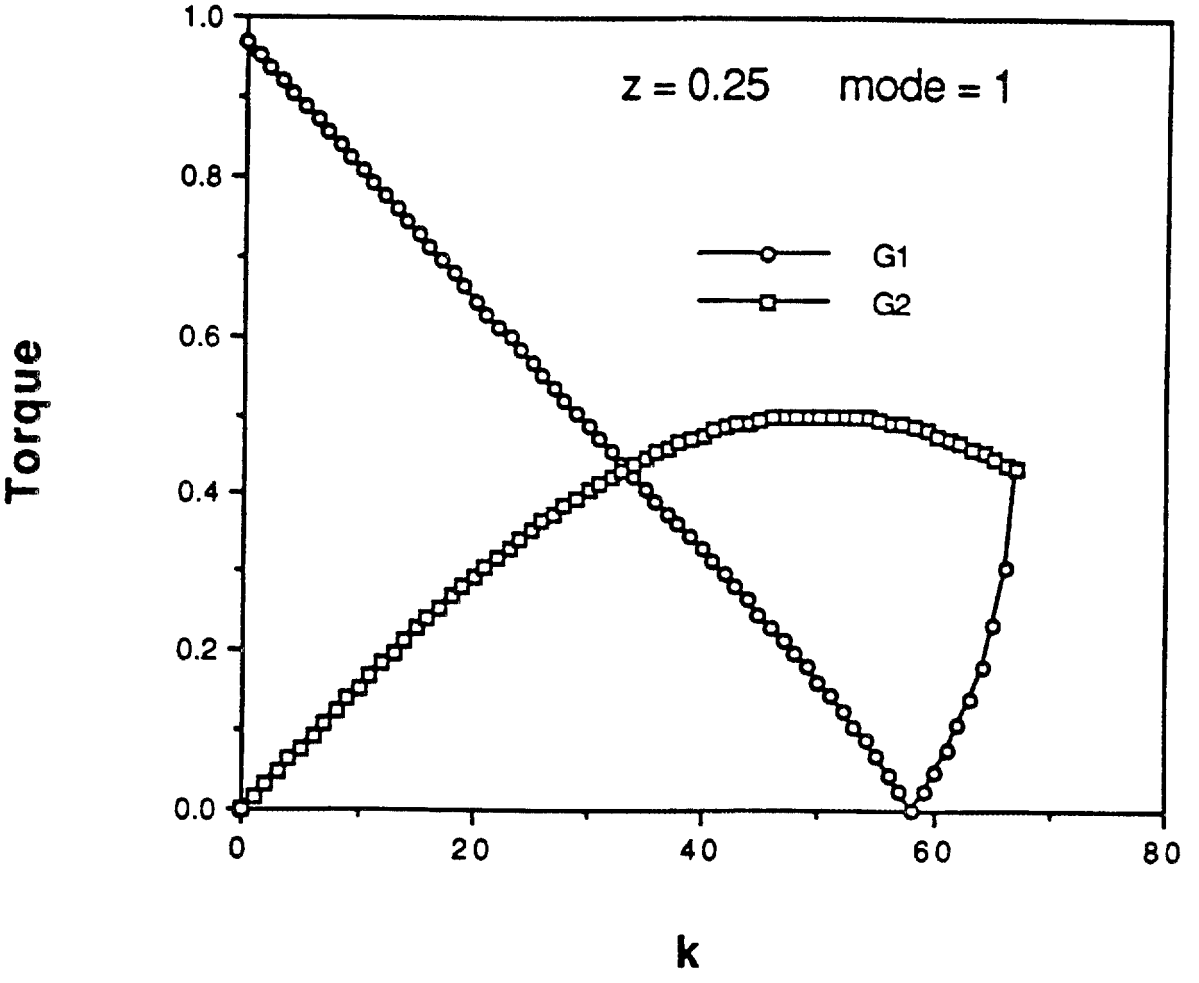

Fig. 6. G^1 and G^2 versus the parameter k for case 3 ($G^2 = G^3$) and mode 1. The units of torque are newton meters.

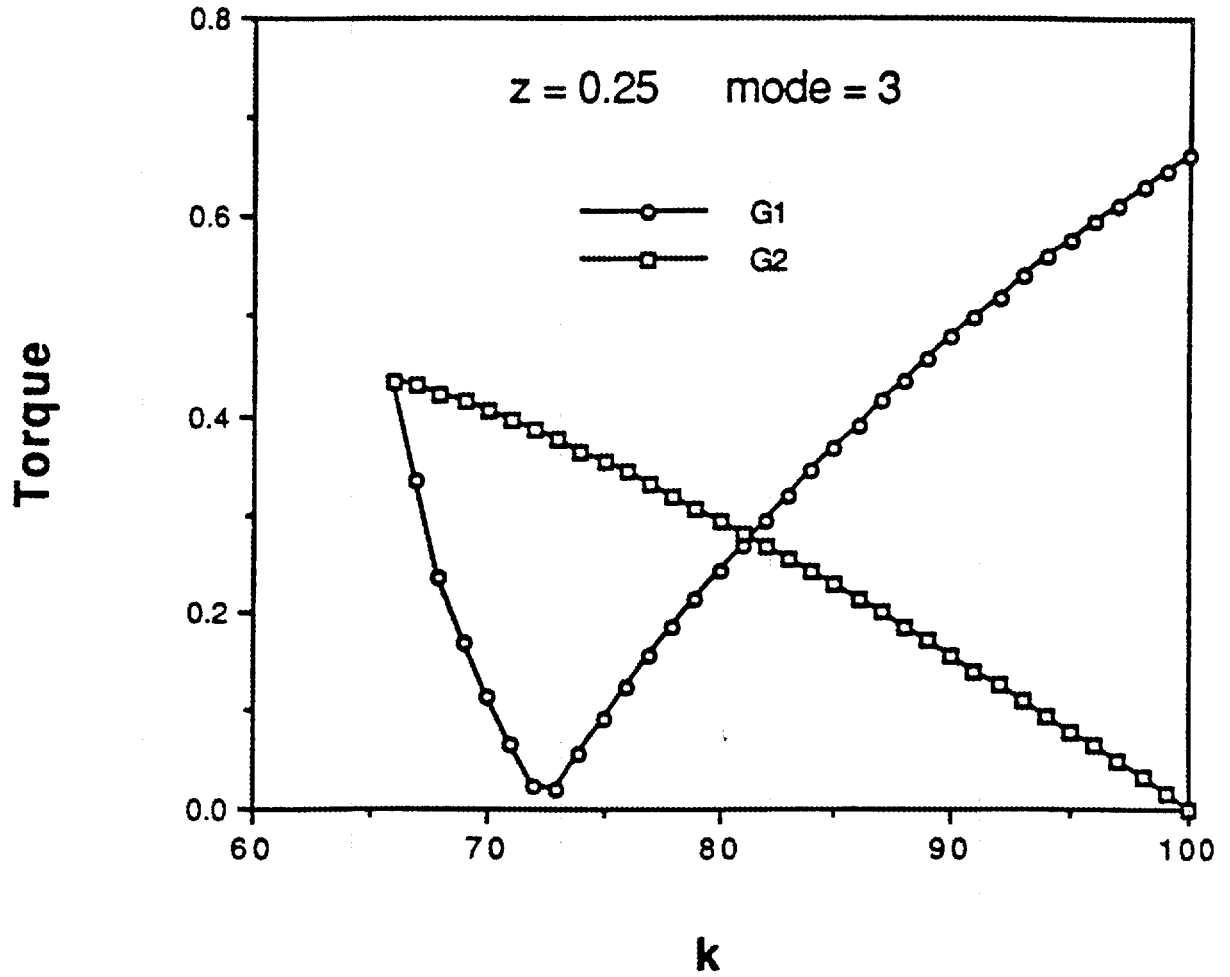

Fig. 7. G^1 and G^2 versus the parameter k for case 3 ($G^2 = G^3$) and mode 3. The units of torque are newton meters.

In Case 4, $\tau_2 = -\tau_3$ and $G^2 = G^3$. G^1 and G^2 are plotted in Fig. 8 for Case 4 and mode 0. In Fig. 8, there are two local minima at k = 45 and k = 67. At k = 45, the subcase is 3.3 and the subcase is 3.1 when k = 67.

G^1 and G^2 are plotted in Fig. 9 for Case 4 and mode 2. In Fig. 9, there are four points where $G^1 = G^2$. Three of the four points are local minima at k = 33, k = 53 and k = 82. The point that is not a local minima is at k = 67. The subcases are: 2.2 at k =33, 3.2 at k =53, 3.4 at k =67, and 2.3 at k =82. In Table 3, we found that subcase 3.4 did not satisfy the necessary conditions. In Fig. 9, we find that subcase 3.4 is not a local minima.

By examining two modes of case 3 and two modes of case 4, we have been able to identify all 10 of the subcases that can reach the point z = 0.25. In 8 of the 10 subcases, we have found a local minima. All of the local minima occurred at points where the torques were equal at all three joints. Thus, we were unable to find any local minima at which only two of the joint torques were equal.

Finally, we shall consider the Class 1 paths. For Class 1, one of the $G^i(\theta)$ is larger than the others and it must satisfy the conditions of classical optimization [Eq. (19)]. The elements of the A matrix are the partial derivatives of the $G^i(\theta)$. If G^1 is largest, the classical optimization conditions require that the first column of the A^T matrix will be zero. If G^2 is largest, the second column of the A^T matrix will be zero and if G^3 is largest, the third column will be zero. In all three cases, $S_3(\theta) = 0$ [see Eq. (34)]. Thus, $\sin \psi_3 = 0$ and $\cos \psi_3 = \pm 1$. Consequently, $G^3 = 0.5$ [see Eq. (28)] and $Q(\theta)$ cannot be less than 0.5. None of the Class 1 paths can be better than the best Class 3 paths in Fig. 5.

The Class 3 paths span the workspace. The local minima for the Class 2 paths occur when they become Class 3 paths. The minimum torque for the Class 1 paths is never less than 0.5 newton meters (the maximum values for the torque on the Class 3 paths).

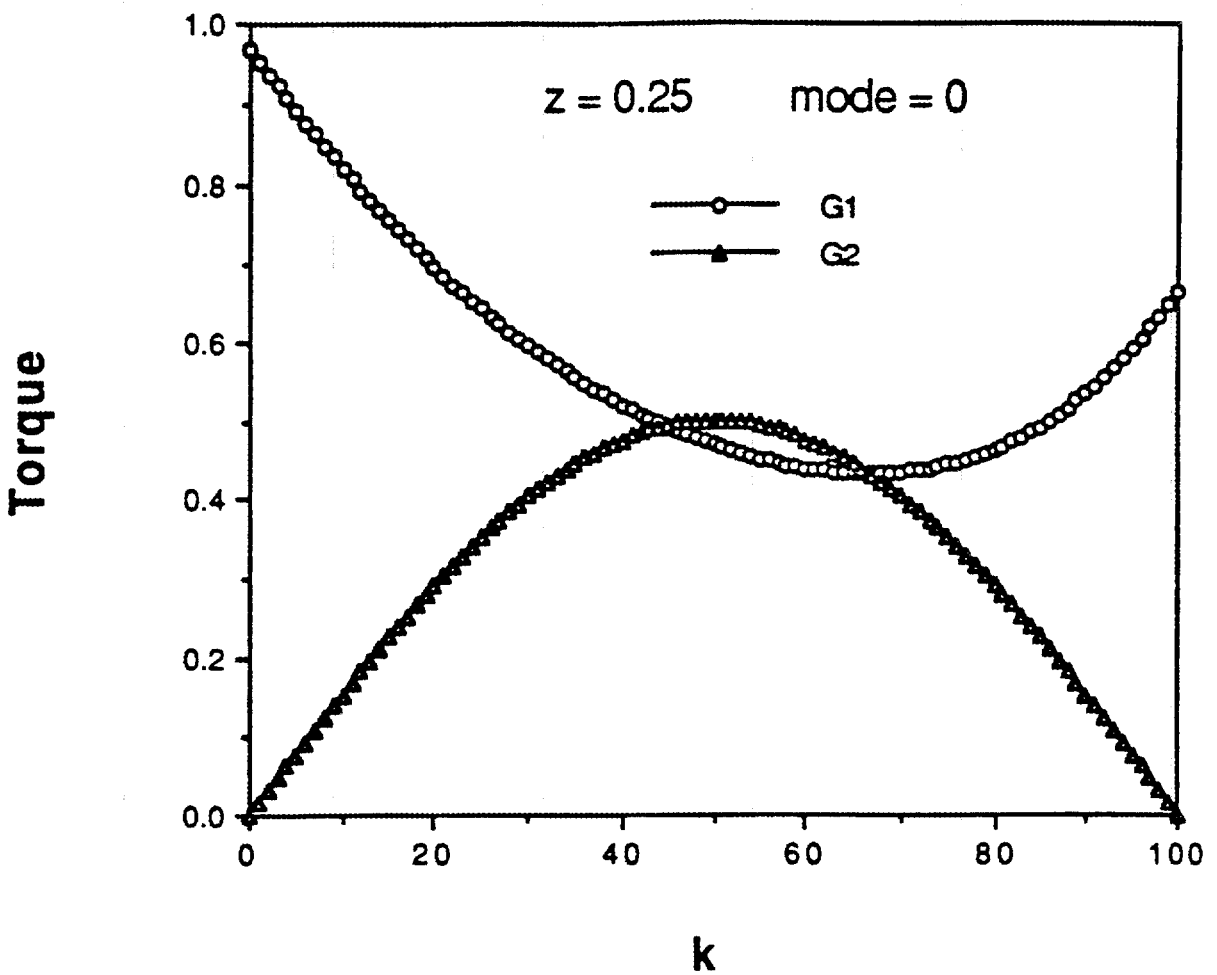

Fig. 8. G^1 and G^2 versus the parameter k for case 4 ($G^2 = G^3$) and mode 0. The units of torque are newton meters.

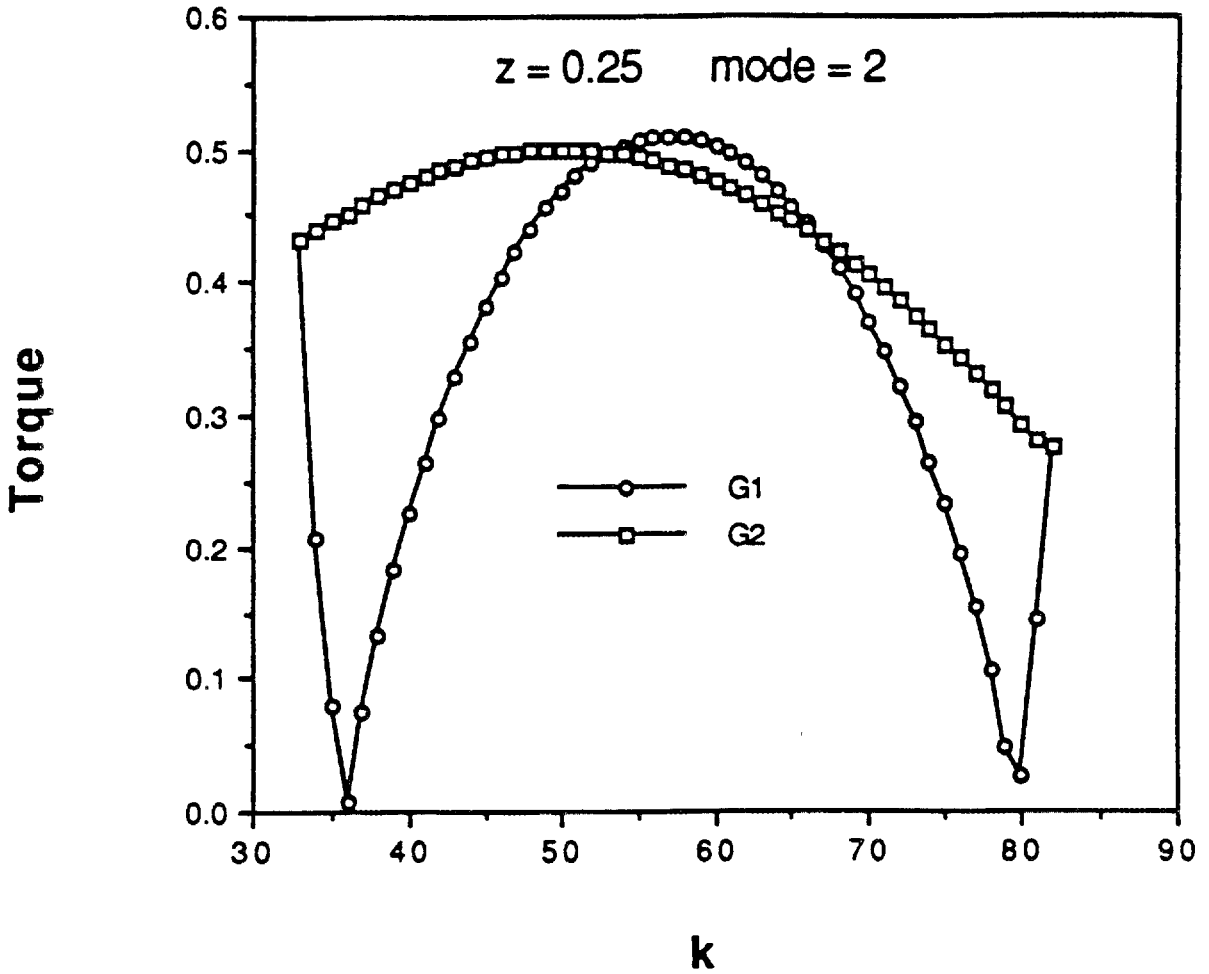

Fig. 9. G^1 and G^2 versus the parameter k for case 4 ($G^2 = G^3$) and mode 2. The units of torque are newton meters.

4. MIN-MAX PATHS FOR CESARm

The CESARm is a manipulator with 7 degrees of freedom (including a 3 degree of freedom spherical wrist) and a high capacity to weight ratio [5] (see Fig. 10). We assume that the CESARm is mounted on a mobile platform. The platform can move in the x and y directions. The manipulator can reach points in three dimensional (x,y,z) space. We assume that the platform will control the x and y coordinate of the arm's tip (P) [we recognize that obstacles could prevent free motion of the platform in the (x,y) plane]. We will not consider the last three degrees of freedom that control the spherical wrist. Since the first joint variable does not change the z coordinate of P, we will neglect it.

The z coordinate of P is given by:

$$z = s_2 c_3 D + c_2 H \tag{44}$$

where $s_i = \sin(\theta_i)$, $c_i = \cos(\theta_i)$, and:

$$D(\theta_4) = a_4 c_4 + a_3 \tag{45}$$

$$H(\theta_4) = a_4 s_4 - d_3 \tag{46}$$

and a_3, a_4, and d_3 are constants ($a_3 = 0.029$ m, $a_4 = 0.508$ m, and $d_3 = 0.635$ m). The components of the Jacobian are:

$$J_2 = c_2 c_3 D - s_2 H \tag{47}$$

$$J_3 = - s_2 s_3 D \tag{48}$$

$$J_4 = - a_4 s_2 c_3 s_4 + a_4 c_2 c_4 \tag{49}$$

If the force is directed downward ($F_z = -1$ newton), the joint torques are given by:

$$\tau_i = - J_i \tag{50}$$

We will assume that the weights for each joint are equal: $w_i = 1$.

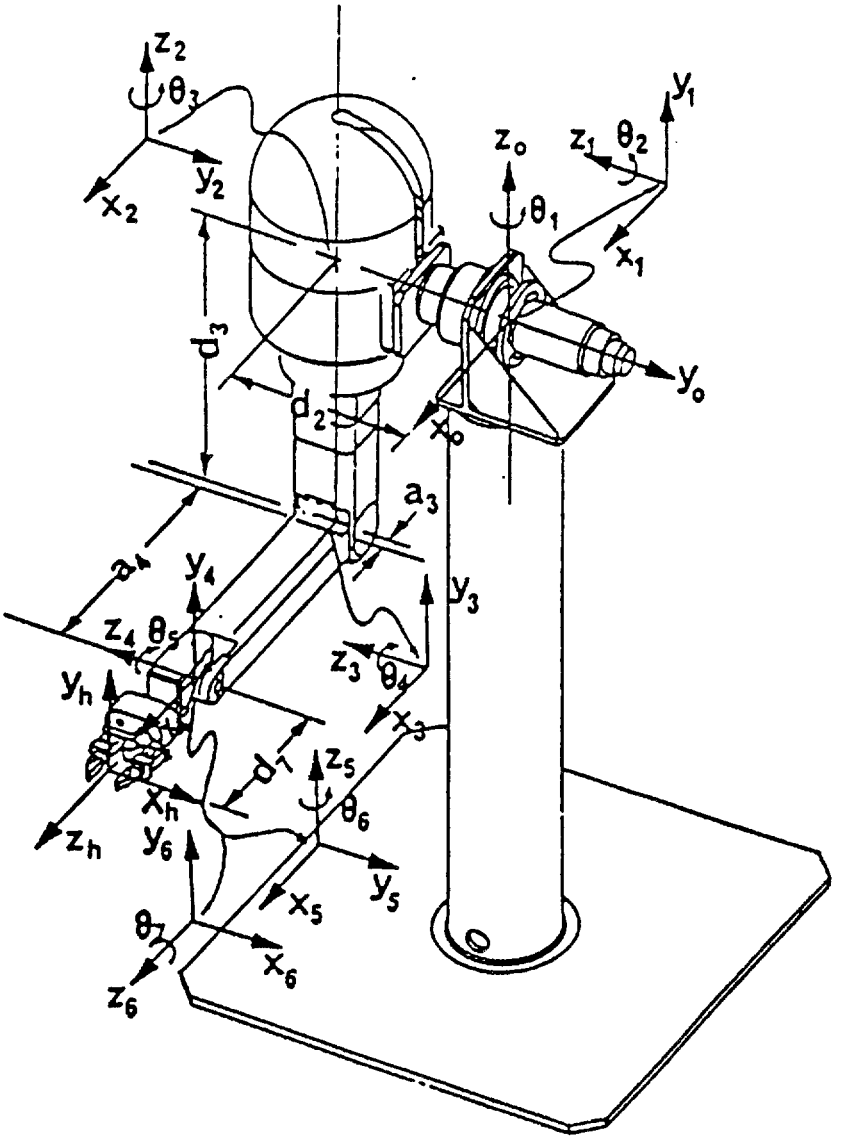

Fig. 10. The seven degrees of freedom of the CESARm manipulator.

We have three joint angles (θ_2, θ_3, θ_4) controlling the height of the arm (z). Given a desired change in height, we would like to determine paths for the joint angles that minimize the maximum of the torque during the motion. In the second section, we demonstrated that at the min-max point the magnitude of the torques will be equal to the min-max value at one or more of the joints. We begin by exploring the Class 3 paths where the magnitudes of all three torques are equal during the motion (subsequently, we will consider the Class 2 paths where two of the three torques are equal and the Class 1 paths). Define K_3 to be the ratio of J_2 and J_3 and K_4 to be the ratio of J_3 and J_4:

$$K_3 = J_2 / J_3 \tag{51}$$

$$K_4 = J_3 / J_4 \tag{52}$$

Since $K_3 = \pm 1$ and $K_4 = \pm 1$, we can distinguish four cases. For the planar manipulator, the four cases were distinct (see Table 1). For the CESARm, we will now show that the four cases correspond to changes of variables (see Table 6).

Table 6. Four sets of joint angles that will reach each (Q,z) point.

Case	K_3	K_4	θ_2	θ_3
1	+ 1	+ 1	θ_2	θ_3
2	+ 1	− 1	$-\theta_2$	$\pi - \theta_3$
3	− 1	− 1	θ_2	$-\theta_3$
4	− 1	+ 1	$-\theta_2$	$-(\pi - \theta_3)$

If the sign of θ_3 is changed, the sign of s_3 changes. Consequently, the signs of z, J_2, and J_4 are unchanged, while the sign of J_3 changes. Thus, the signs of both K_3 and K_4 change (case 3).

If the sign of θ_2 is changed and θ_3 is replaced by (π - θ_3), the signs of s_2 and c_3 change. Consequently, the signs of z and J_4 are unchanged, while the signs of J_2, and J_3 change. Thus, the sign of K_4 changes (case 2).

If the sign of θ_2 is changed and θ_3 is replaced by -(π - θ_3), the signs of s_2, s_3, and c_3 change. Consequently, the signs of z, J_3, and J_4 are unchanged, while the sign of J_2 changes. Thus, the sign of K_3 changes (case 4).

Since the four cases are not distinct, we assume that $K_3 = K_4 = 1$. We have two equations in three unknowns. For each pair of equations, we can solve for $T_2 = \tan \theta_2$:

$$T_2 = c_3 D / (H - s_3 D) \tag{53}$$

$$T_2 = a_4 c_4 / (a_4 c_3 s_4 - s_3 D) \tag{54}$$

We can eliminate θ_2 and obtain a single equation relating θ_3 and θ_4:

$$a_4 c_4 (H - s_3 D) = c_3 D (a_4 c_3 s_4 - s_3 D) \tag{55}$$

Using a step size of 2 degrees, we allow θ_4 to sweep its allowable range (from -55 degrees to 45 degrees). At each step, θ_4 is known and we use a search technique (Brent's method. See Press [6]) to find all of the values of θ_3 that satisfy Eq. (55) (when θ_4 is known, we have replaced a two parameter (θ_2 and θ_3) search of a function that does not have a continuous derivative [Eq. (6)] by a one parameter search of a function with a continuous derivative). The results are displayed in Fig. 11.

As θ_4 increases from -55 degrees, there are no solutions of Eq. (55) until θ_4 reaches -9 degrees. When $\theta_4 = -9$ degrees, there are two solutions with positive z: (z,Q) = (0.73, 0.30) and (z,Q) = (0.67, 0.33). The two solutions with negative z correspond to an increase in θ_2 by 180 degrees. When z is positive (or negative), we can separate the paths in Fig. 11 into two distinct paths that have continuous values of the joint variables: upper and lower. The upper path begins at (z,Q) = (0.67, 0.33) and extends to point B [(z,Q) = (0.17, 0.24)]. The lower path begins at (z,Q) = (0.73, 0.30) and extends to point A [(z,Q) = (0.29, 0.27). The maximum value of Q on the upper path is 0.37, while all of the values on the lower path are less than 0.30. The left ends of the two paths (when z is positive) occur when θ_4 is at its upper limit (45 degrees).

Our goal is to determine continuous paths for the joint variables that will minimize Q during a large scale vertical motion by the mobile manipulator. Although the upper path has a greater range in z and a lower values for Q at its left end, the lower path is more attractive for large scale motions because it has a smaller maximum value for Q. In the remainder of this section, we will consider both of the equal paths: upper and lower.

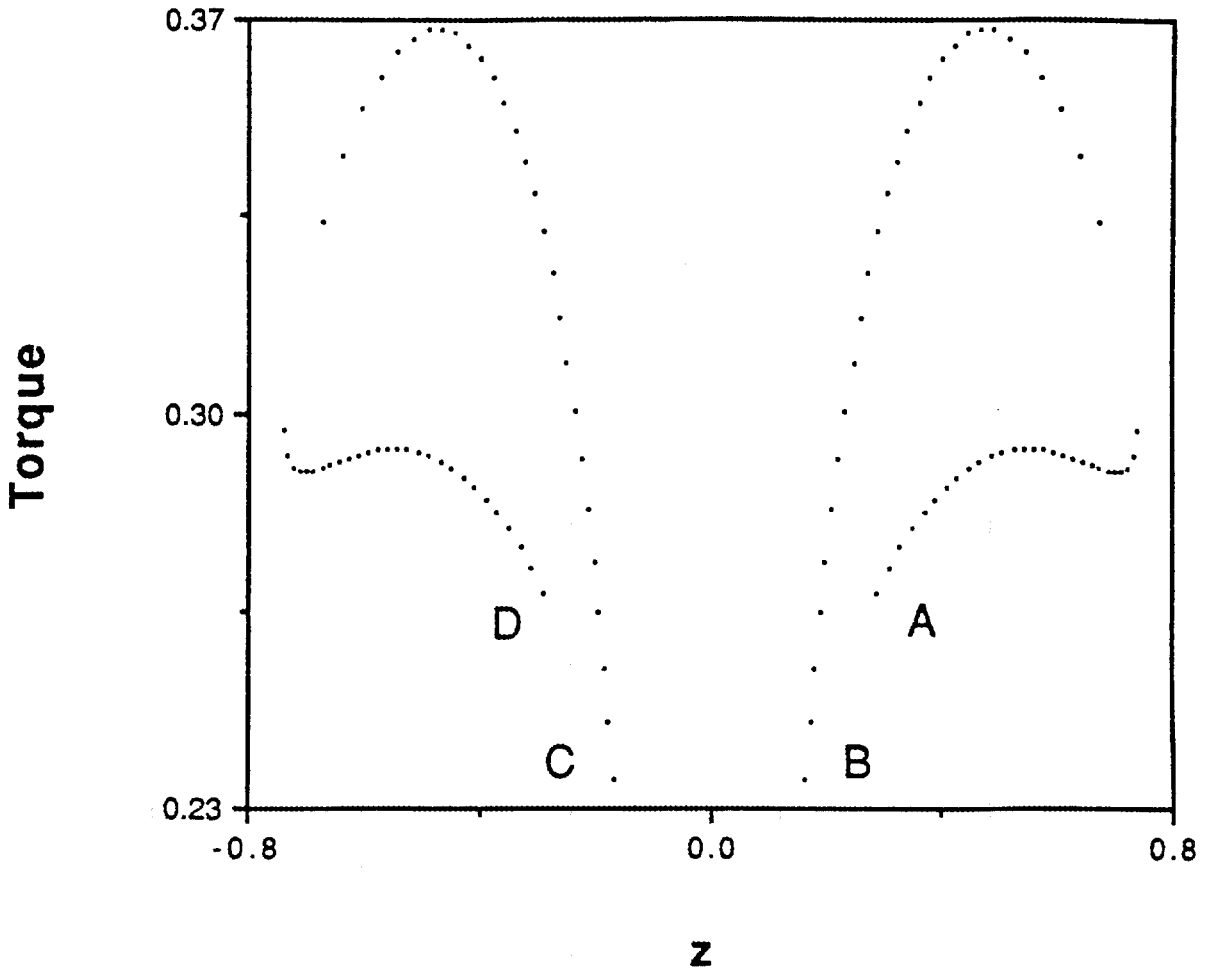

Fig. 11. Maximum torque (Q) versus height (z) for paths with three equal torques. The units of torque are newton meters and the units of height are meters.

The two segments of the equal paths are the only Class 3 solutions and they cannot reach all of the workspace for the CESARm. To cover all of the workspace, we will use Class 2 solutions. To define the workspace of the CESARm, we will introduce two new variables (R and α) and derive a new expression for the z coordinate of the CESARm. We express the variables c_3 D and H in polar coordinates:

$$c_3 D = R \sin \alpha \tag{56}$$

$$H = R \cos \alpha \tag{57}$$

where:

$$R^2 = (c_3 D)^2 + H^2 \tag{58}$$

$$\tan \alpha = c_3 D / H \tag{59}$$

Using Eqs. (56) and (57), Eq. (44) may be written:

$$z = R \cos(\theta_2 - \alpha) \tag{60}$$

As θ_2 increases from α to $\alpha + \pi$, z will decrease from R to -R. Thus, R defines the reach for the CESARm. For fixed values of θ_4 (D and H), the maximum value of R will occur when $c_3 = \pm 1$ and $\theta_3 = 0$ or π.

In Fig. 12, values of Q are plotted for three cases as θ_2 increases from α to $\alpha + \pi$. For the cases in Fig. 12, $\theta_3 = 0$ and θ_4 = -55 degrees, -5 degrees, and 45 degrees. The maximum value of the reach occurs when θ_4 = -55 degrees and R = 1.10 meters. The case when θ_4 = -55 degrees has very high values for Q when z = 0. The case when θ_4 = 45 degrees has much lower values for Q in the neighborhood of z = 0. For the cases in Fig. 12, a good strategy for moving through the workspace would be to move from the maximum reach posture (θ_4 = -55 degrees) to the minimum reach posture (θ_4 = 45 degrees) and back to the maximum reach posture as the elevation of the CESARm moves from 1.10 meters to -1.10 meters.

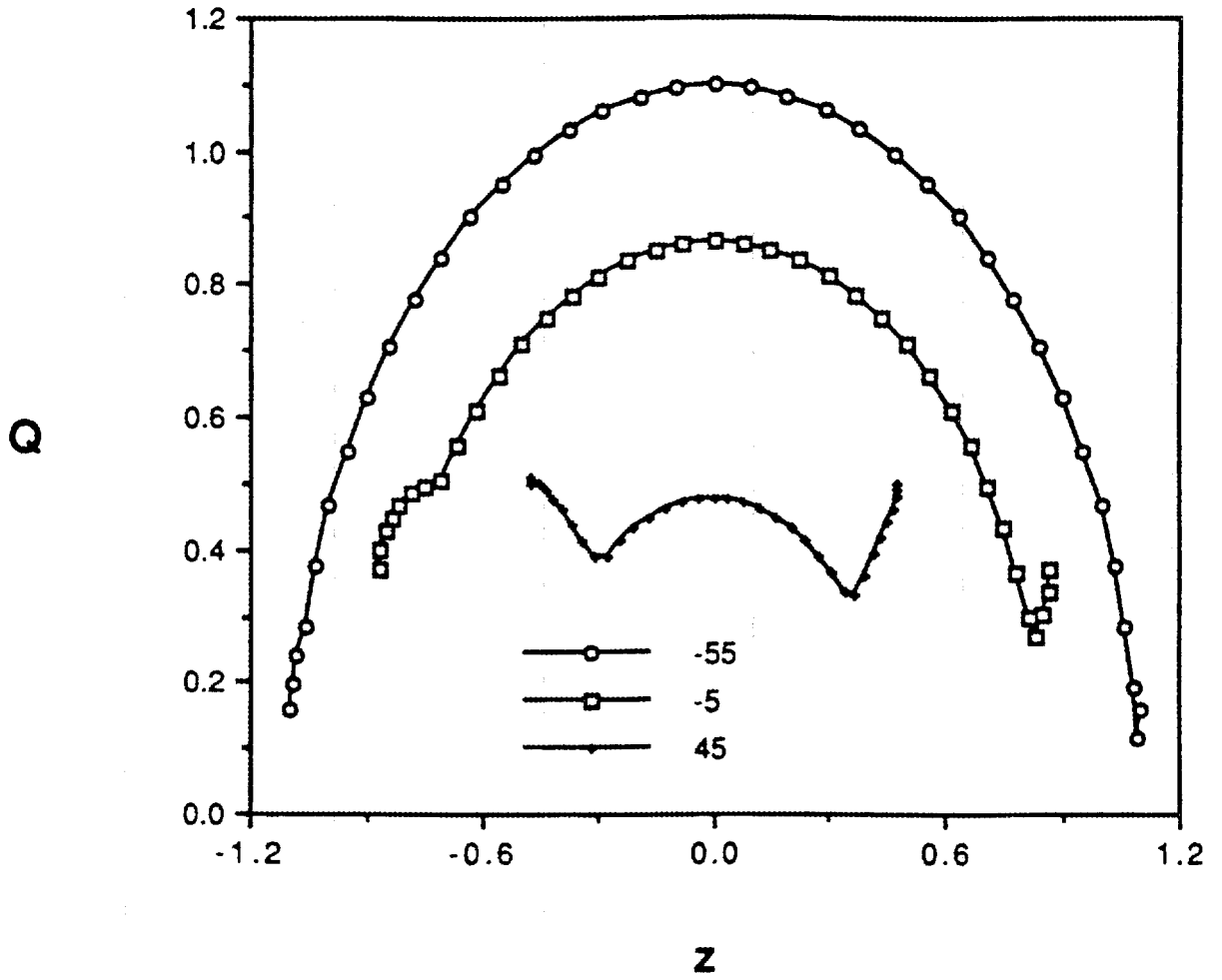

Fig. 12. Maximum torque (Q) versus height (z) for three values of θ_4. The units of torque are newton meters and the units of height are meters .

In each of the three cases displayed in Fig. 12, the plots of Q vs z have local minima. The local minima are Class 2 solutions that occur when the maximum torque switches from one joint to another. Since $\theta_3 = 0$, $J_3 = 0$ [see Eq. (48)]. Thus, the local minima always occur when $G^2(\theta) = G^4(\theta)$ or $J_2 = \pm J_4$. For each value of θ_4 there are two values of θ_2 (and two values of z) for which $G^2(\theta) = G^4(\theta)$. In Fig. 12, the solutions with positive values of z have lower values than the solutions with negative values of z.

The branch with the lower values is plotted in Fig. 13 (and labeled Long). The lower path from Fig. 11 is plotted in Fig. 13 (and labeled Equal). The Long path has a greater range than the Equal path. Furthermore, the Long path has lower values for Q for values of z that are greater than the value at which the two curves cross (although the curves cross in Fig. 13, the joint angles are not equal. $\theta = (110, 0, 15)$ for Long and $\theta = (-121, -140, 5)$ for Equal). The Equal path has lower values for Q for values of z that are less than the value at which the two curves cross.

By exploring Class 2 paths, we have found a continuous path that could reach larger values of z than the Class 3 Equal path. Next, we will seek Class 2 paths that can bridge between the two segments of the Long path or the four segments of the Equal path.

A bridge path must be continuous in joint space. For each point in a plot of Q and z, there are four sets of joint angles that will reach the point. Consider the surface of Q as a function of θ_2 and θ_3. We will keep θ_4 constant ($\theta_4 = 45$ degrees). From Table 6, we find the surface is symmetrical about the θ_2 axis [since $Q(\theta_2, -\theta_3) = Q(\theta_2, \theta_3)$, the surface is symmetrical about the line where $\theta_3 = 0$ (the θ_2 axis)]. Since the surface is symmetrical, we will assume that the values of θ_3 lie between 0 and π. The surface is not symmetrical about the θ_3 axis [$Q(-\theta_2, \pi-\theta_3) = Q(\theta_2, \theta_3)$. We will assume that the values of θ_2 lie between $-\pi$ and π. Thus, there will be two sets of joint angles that will reach each (Q,z) point The set with positive values for θ_2 will be called set one, while the set with negative values for θ_2 will be called set two.

To find Class 2 paths, we seek all values of the joint angles that have equal magnitudes for two of the three torques. With θ_4 constant ($\theta_4 = 45$ degrees), we vary θ_2 from -180 degrees to 180 degrees. For each value of θ_2, we find all of the values for θ_3 that have equal magnitudes for two of the three torques. For each value of θ_2, there can be as many as six values for θ_3 ($J_2 = \pm J_3$, $J_2 = \pm J_4$, and $J_3 = \pm J_4$. The six expressions for θ_3 are derived in the appendix). When two of the three torques have equal magnitudes ($G^i = G^j$), the third torque (G^k) can be larger or smaller than the two equal torques. We restrict our attention to the case where the two equal torques are larger than the third torque and consequently are on the Q surface.

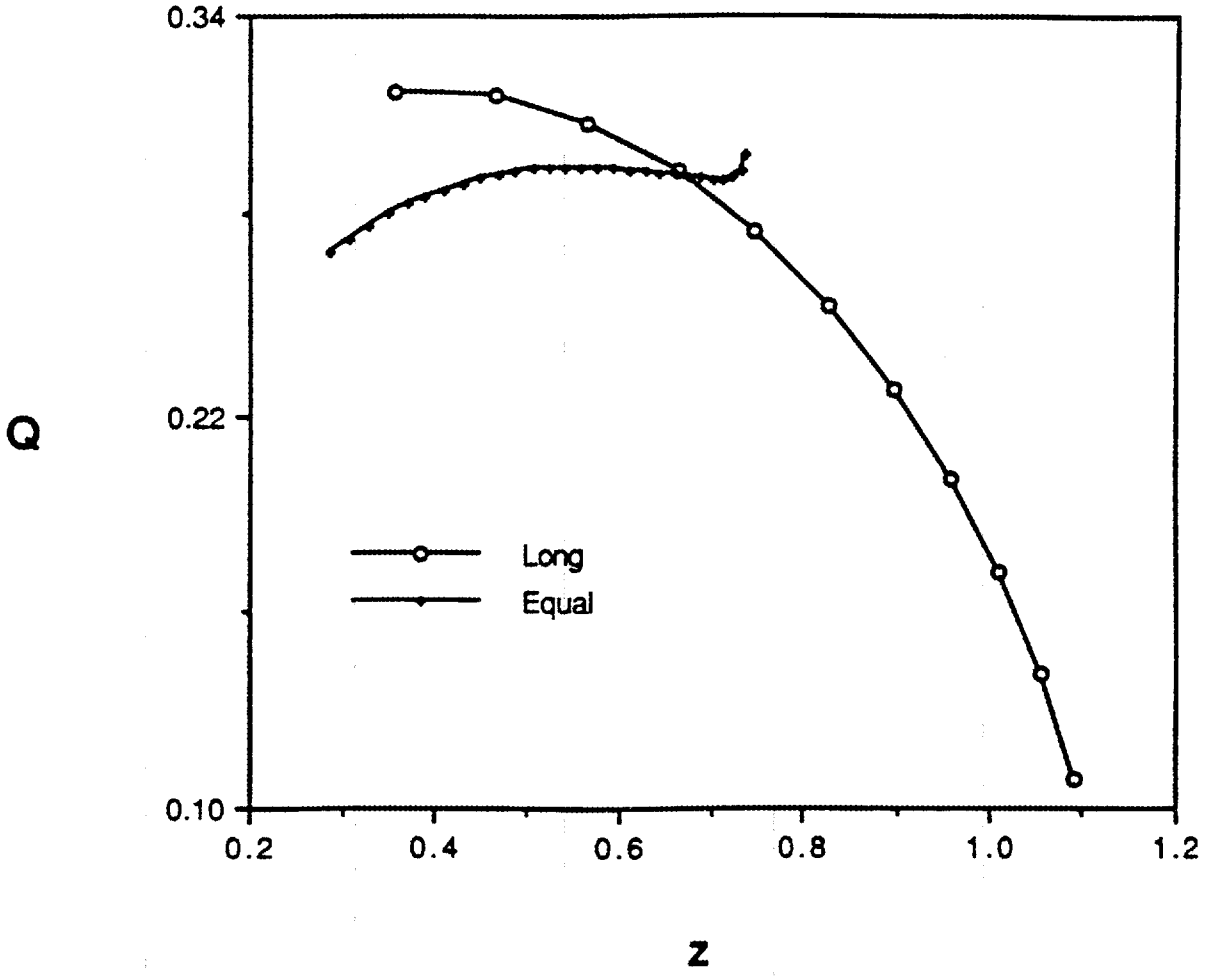

Fig. 13. Maximum torque (Q) versus height (z) for the Long path and the Equal path. The units of torque are newton meters and the units of height are meters.

To discuss the paths on the Q surface, we will define the beginning and ending points for the paths. In Fig. 11, we identified the four segments of the Equal path using the letters A, B, C, and D. For each point on a bridge path, there will be two sets of joint angles. At point A, the set with positive values for θ_2 will be called A_1, while the set with negative values for θ_2 will be called A_2. Our list of significant points on the bridge paths is given in Table 7.

Fig. 14 is a network diagram showing the connections between the significant points on the bridge paths that are defined in Table 7. Although all of the points are displayed in the correct positions, the paths between the points are not the straight lines in Fig. 14. We have previously discussed the points A, B, C, and D. The points E and F are on the boundary between positive and negative values of θ_2 (recall that the angle $\theta_2 = \pi$ is equal to the angle $\theta_2 = -\pi$). The points G and H are the ends of the two segments of the Long path. Furthermore, G and H are on the boundary between positive and negative values of θ_3. The points J, K, L, and M are intermediate points on a bridge paths between the four ends of the segments of the Equal path at which the torque attains its maximum value (they are the summits on the paths).

In Fig. 14, there are two paths from A to D: AJC and CMD or ALB and BKD. Both paths have the same maximum value for Q (at points J or K). Similarly, there are two paths from B to C. The path from A to B via L has a lower value for Q than the path via J, C, M, D, and K. The path from G to H passes through A and D.

For each point on the surface of Q in the Q-z plane, there are two sets of joint angles with positive values for θ_3 (and two sets of joint angles with negative values for θ_3) that will reach the point. The network diagram showing the bridge path connections in the Q-θ_2 plane is displayed in Fig. 15, while the network diagram in the Q-θ_3 plane is displayed in Fig. 16. In Fig. 15, the points with positive values for θ_2 have the subscript one, while the points with negative values for θ_2 have the subscript two. The points E and F are on the boundary between positive and negative values of θ_2. In Fig. 16, we see that all significant values of θ_3 have two points; the first with the subscript one and the second with the subscript two. There is a path between the points E_1 and E_2 and between the points F_1 and F_2. Thus, the points E and F provide paths between the subscript one points and the subscript two points (paths between positive and negative values of θ_2).

We have reviewed the connection network for the bridge paths. Next, we will learn the topography of the Q surface by examining slices through the surface for various positive values of θ_2. We begin with $\theta_2 = 0$ (see Fig. 17). From Table 6, we expect the figure to be symmetrical about $\theta_3 = 90$ degrees [since, $Q(\theta_3) = Q(\pi - \theta_3)$]. From Fig. 15,

we expect to see point F in this figure. Point F_1 is when $G^2 = G^4$ at 22 degrees, while point F_2 is when $G^2 = G^4$ at 158 degrees. Since Q is constant between F_1 and F_2, there is no torque penalty in moving from F_1 to F_2. Point F_1 is the trailhead for the path to positive values of θ_2, while F_2 is the trailhead for the path to negative values of θ_2.

Table 7. The joint angles at the significant points on the bridge paths.

Point	z	Q	θ_2	θ_3
A_1	0.29	0.27	91	44
A_2	0.29	0.27	−91	136
B_1	0.17	0.24	142	102
B_2	0.17	0.24	−142	78
C_1	−0.17	0.24	38	78
C_2	−0.17	0.24	−38	102
D_1	−0.29	0.27	89	136
D_2	−0.29	0.27	−89	44
E_1	0.28	0.36	180	158
E_2	0.28	0.36	−180	22
F_1	−0.28	0.36	0	22
F_2	−0.28	0.36	0	158
G_1	0.36	0.32	84	0
G_2	0.36	0.32	−84	180
H_1	−0.36	0.32	96	180
H_2	−0.36	0.32	−96	0
J_1	0.08	0.32	70	62
J_2	0.08	0.32	−70	118
K_1	−0.08	0.32	110	118
K_2	−0.08	0.32	−110	62
L_1	0.28	0.31	115	62
L_2	0.28	0.31	−115	118
M_1	−0.28	0.31	65	118
M_2	−0.28	0.31	−65	62

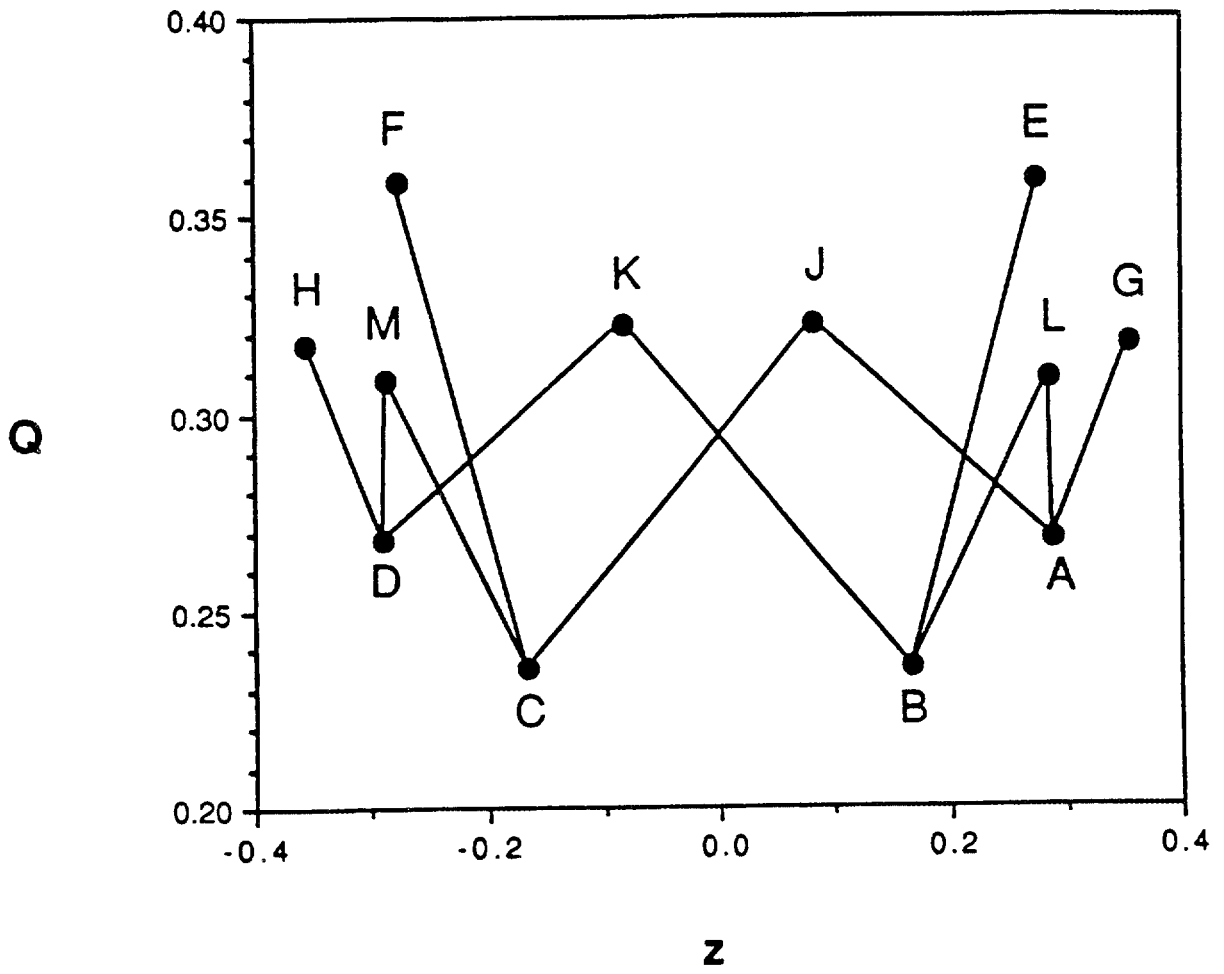

Fig. 14. Network diagram for the Bridge paths. Maximum torque (Q) versus height (z). The units of torque are newton meters and the units of height are meters.

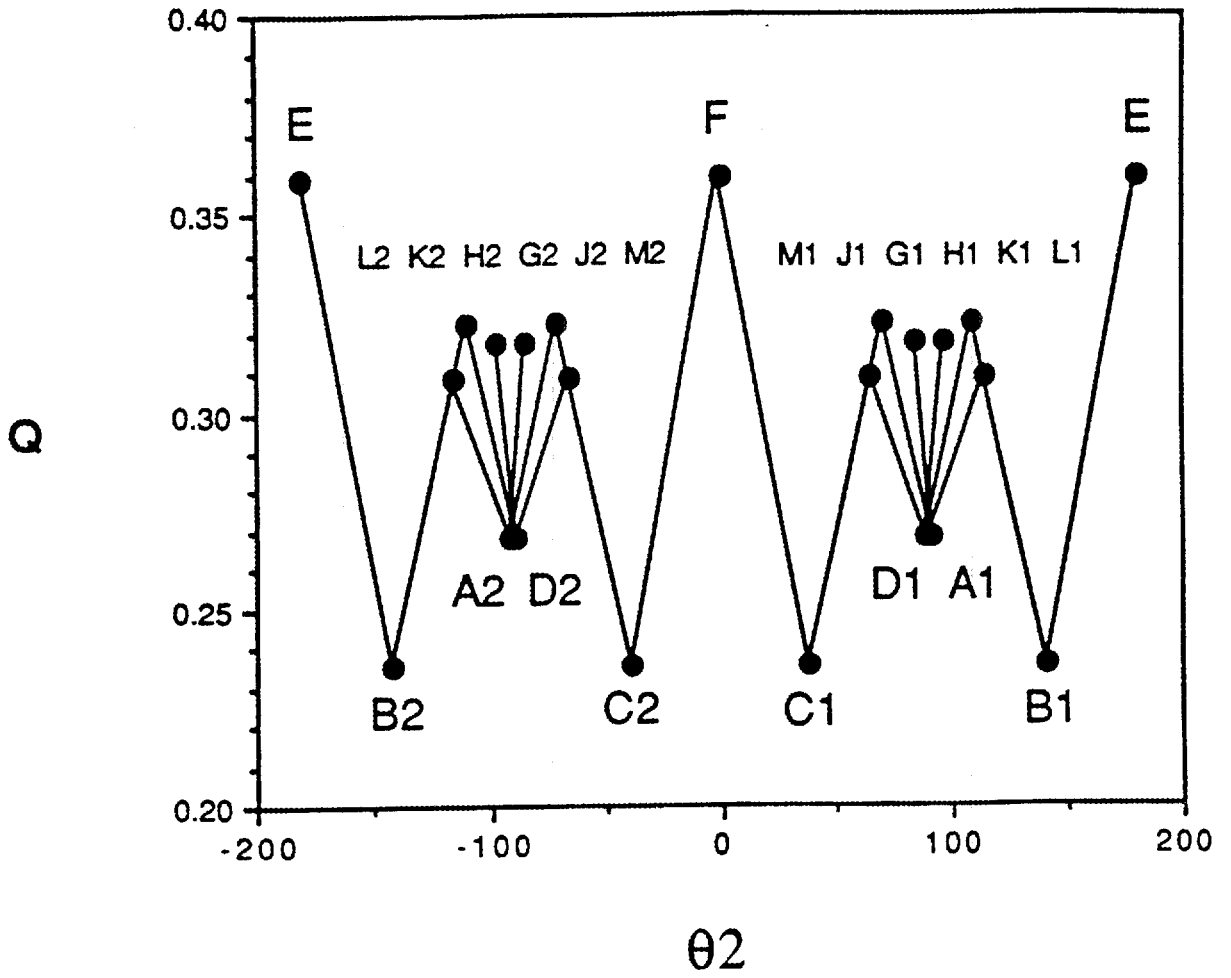

Fig. 15. Network diagram for the Bridge paths. Maximum torque (Q) versus angle (θ_2). The units of torque are newton meters and the units of angle are degrees.

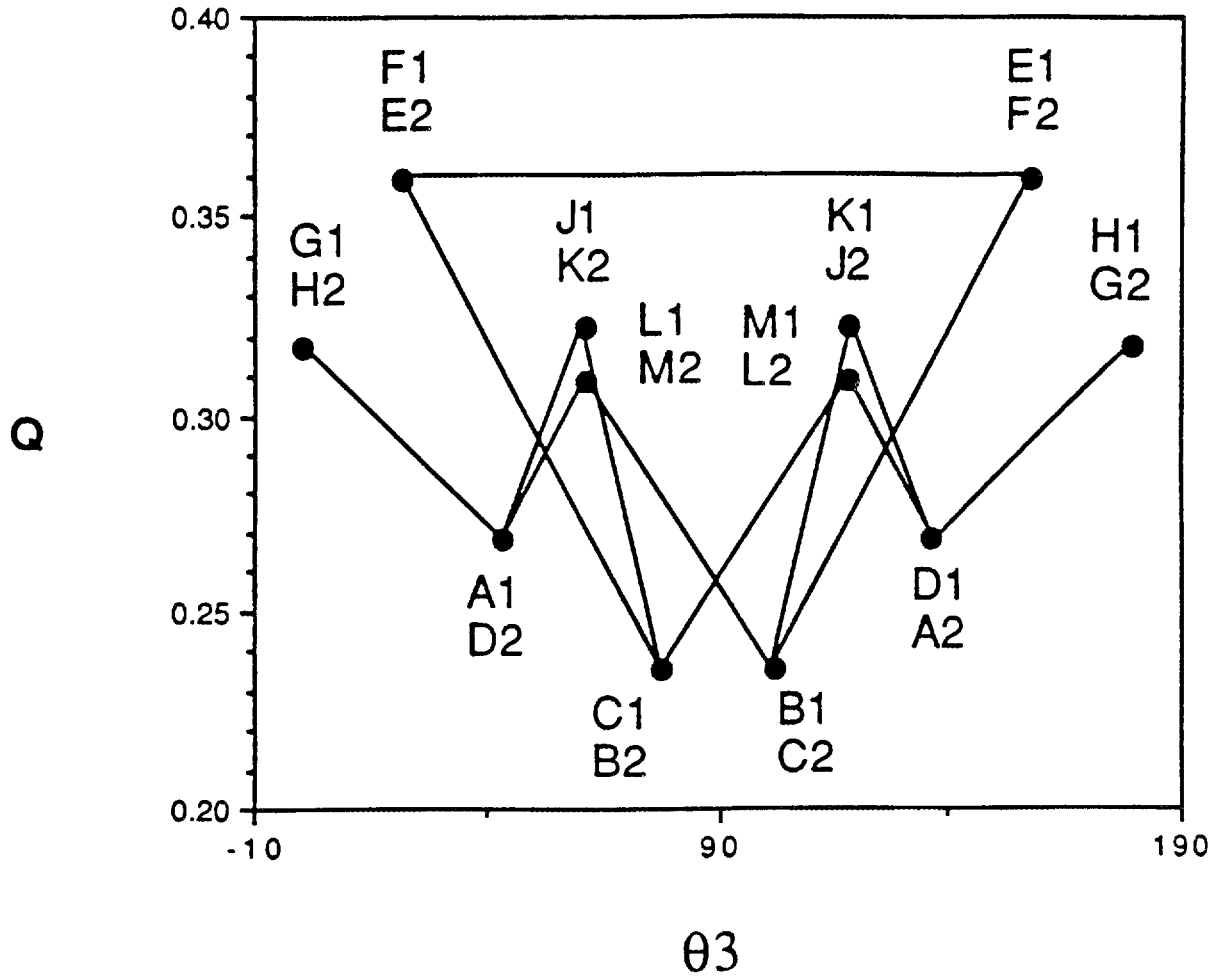

Fig. 16. Network diagram for the Bridge paths. Maximum torque (Q) versus angle (θ_3). The units of torque are newton meters and the units of angle are degrees.

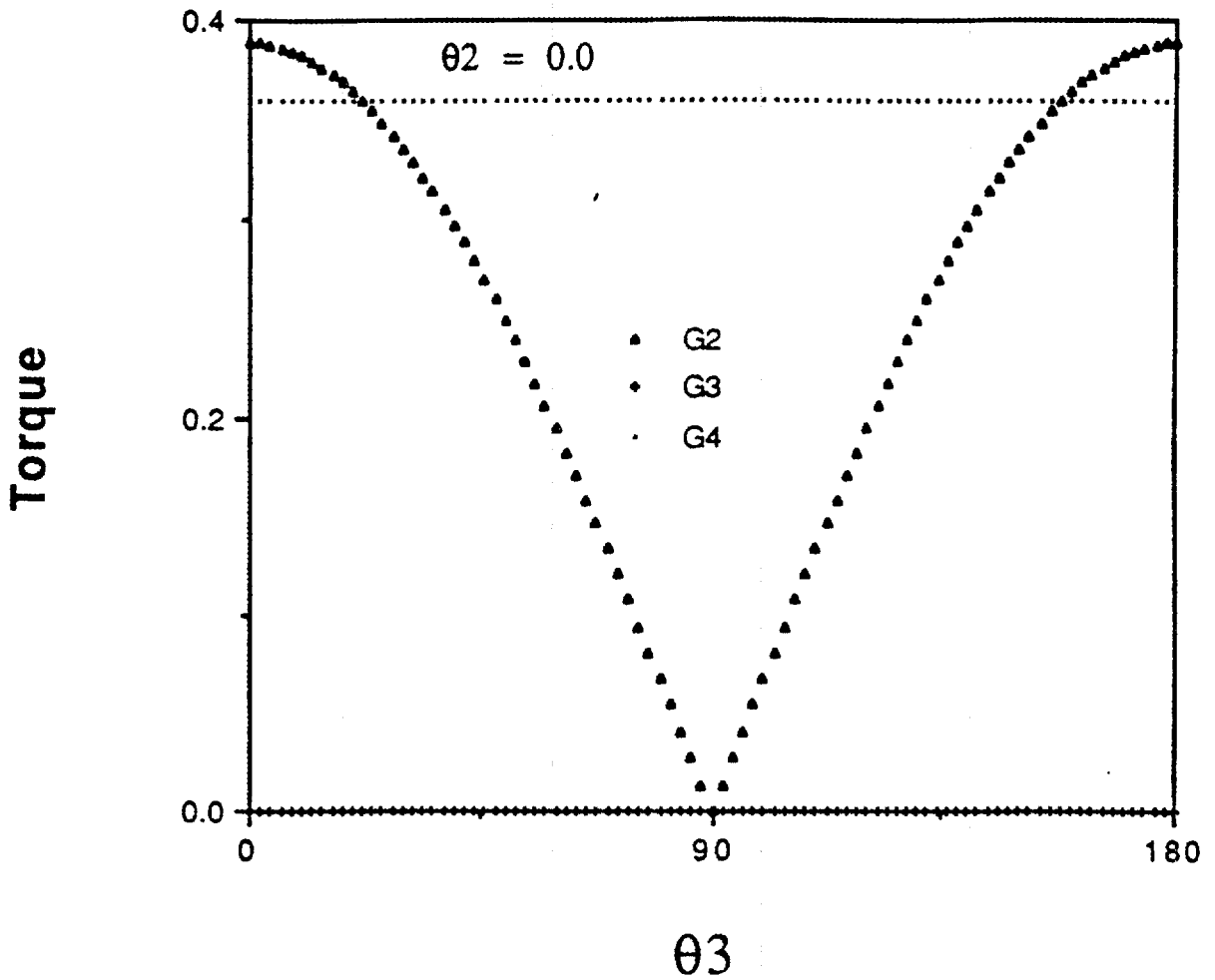

Fig. 17. Maximum torque (Q) versus angle (θ_3) when $\theta_2 = 0$ and $\theta_4 = 45$. The units of torque are newton meters and the units of angle are degrees.

The point C_1 is a Class 3 point where $G^2 = G^3 = G^4$ (see Fig. 18). There is only one path from F_1 to C_1. As θ_2 increases from 38 degrees after C_1, the trail forks and there are two paths: C_1 to A_1 and C_1 to D_1.

The point G_1 is end of the Long path (see Fig. 19). In Fig. 19, $\theta_2 = 83.6$ degrees, G_1 is a local maxima of Q, and the local minima of Q occur at $\theta_3 = 51$ degrees on the path from C_1 to A_1 and at $\theta_3 = 133$ degrees on the path from C_1 to D_1. In Fig. 19, there are six points where $G^i = G^j$. The Q surface is symmetrical about $\theta_3 = 0$ and G_1 is a trailhead for entering the negative values of θ_3. In the network diagram (Fig. 14), the path leads from G_1 to A_1. However, there is not a torque penalty to immediately move from G_1 to the path from C_1 to A_1.

In Fig. 20, $\theta_2 = 88.5$ degrees and the point D_1 is a Class 3 point. We followed the path from C_1 to D_1. As θ_2 increases, two paths leave D_1; one travels to H_1 and the other travels to B_1. Thus, a Class 3 point is the junction of three Class 2 paths. All four Class 3 points in Fig. 14 have this property. On the left side of Fig. 20, we see two Class 2 paths approaching A_1: the path from C_1 to A_1 and the path from G_1 to A_1.

In Fig. 21, $\theta_2 = 91.5$ degrees and the point A_1 is a Class 3 point. As θ_2 increases, the only path leaving A_1 travels to B_1. On the right side of Fig. 21, we see two Class 2 paths leaving D_1: the path from D_1 to B_1 and the path from D_1 to H_1. In both Figs. 20 and 21, we see that there is a hill that prevents a low torque path directly from A_1 to D_1.

In Fig. 22, $\theta_2 = 96.4$ degrees and the point H_1 is end of the Long path. Since the Q surface is symmetrical about $\theta_3 = 0$, H_1 is a local maxima and a trailhead for entering the negative values of θ_3. In Fig. 23, $\theta_2 = 116$ degrees and the point L_1 has the maximum torque on the path from A_1 to B_1.

In Fig. 24, $\theta_2 = 142$ degrees and the point B_1 is a Class 3 point. As θ_2 increases, the only path leaving B_1 travels to E_1.

In Fig. 25, $\theta_2 = 180$ degrees and we have reached point E, the gateway to negative values of θ_2. Like Fig. 17, Fig. 25 is symmetrical about $\theta_3 = 90$ degrees. Point E_1 is at 158 degrees, while point E_2 is at 22 degrees. Since Q is constant between E_1 and E_2, there is no torque penalty in moving from E_1 to E_2. Point E_1 is the trailhead for the path to positive values of θ_2, while E_2 is the trailhead for the path to negative values of θ_2.

We have proven that at the min-max point the magnitude of the normalized torques will be equal to the min-max value at one or more of the joints. We have assumed that the paths with minimal torque will be Class 3 paths that have equal torque in all joints. To extend the space of possible paths, we have considered Class 2 paths. To find paths, we have ignored the position constraint [$f(\theta) = P^*$]. We have found all Class 3 and Class 2 points and then examined their positions.

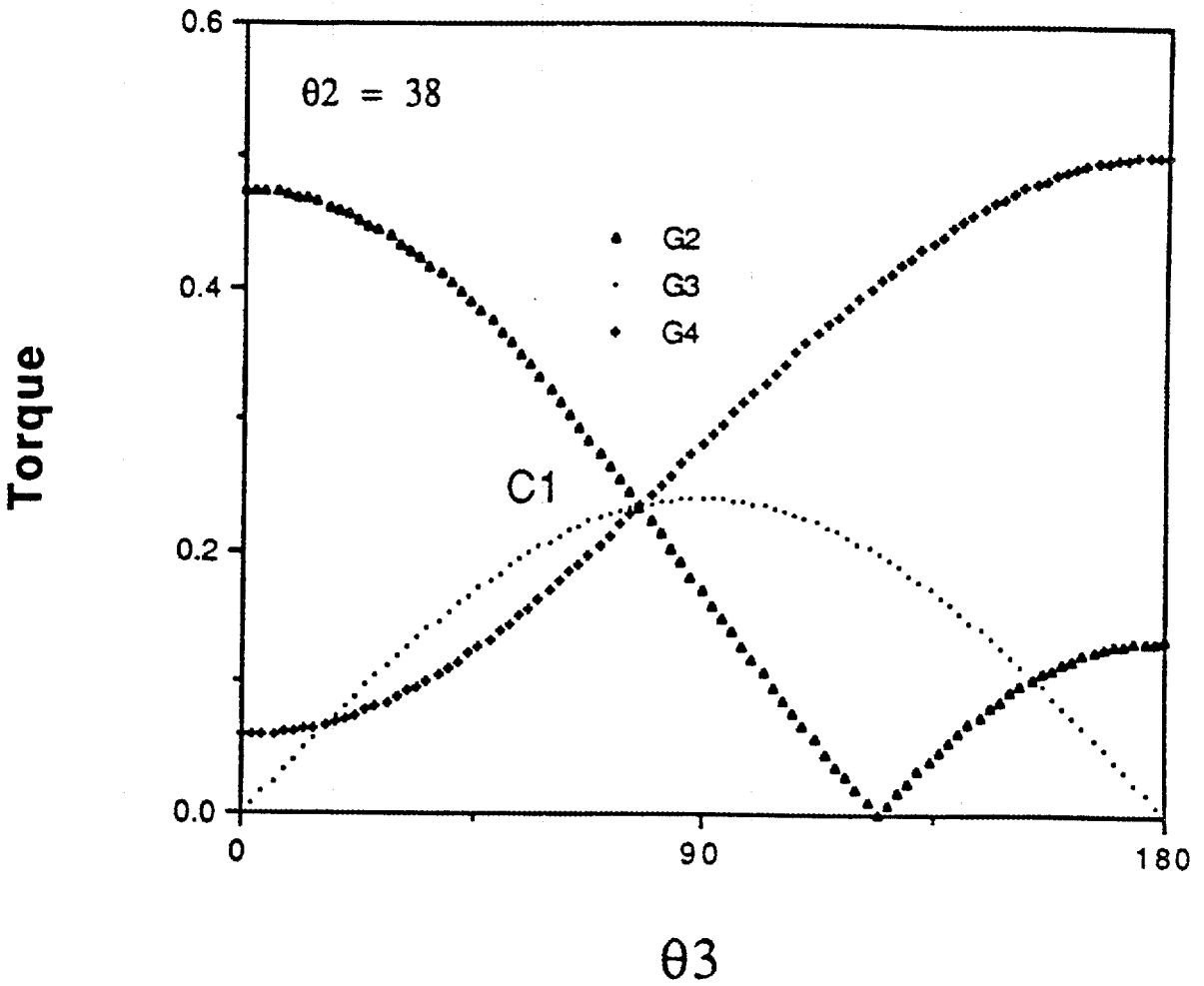

Fig. 18. Maximum torque (Q) versus angle (θ_3) when θ_2 = 38 and θ_4 = 45. The units of torque are newton meters and the units of angle are degrees.

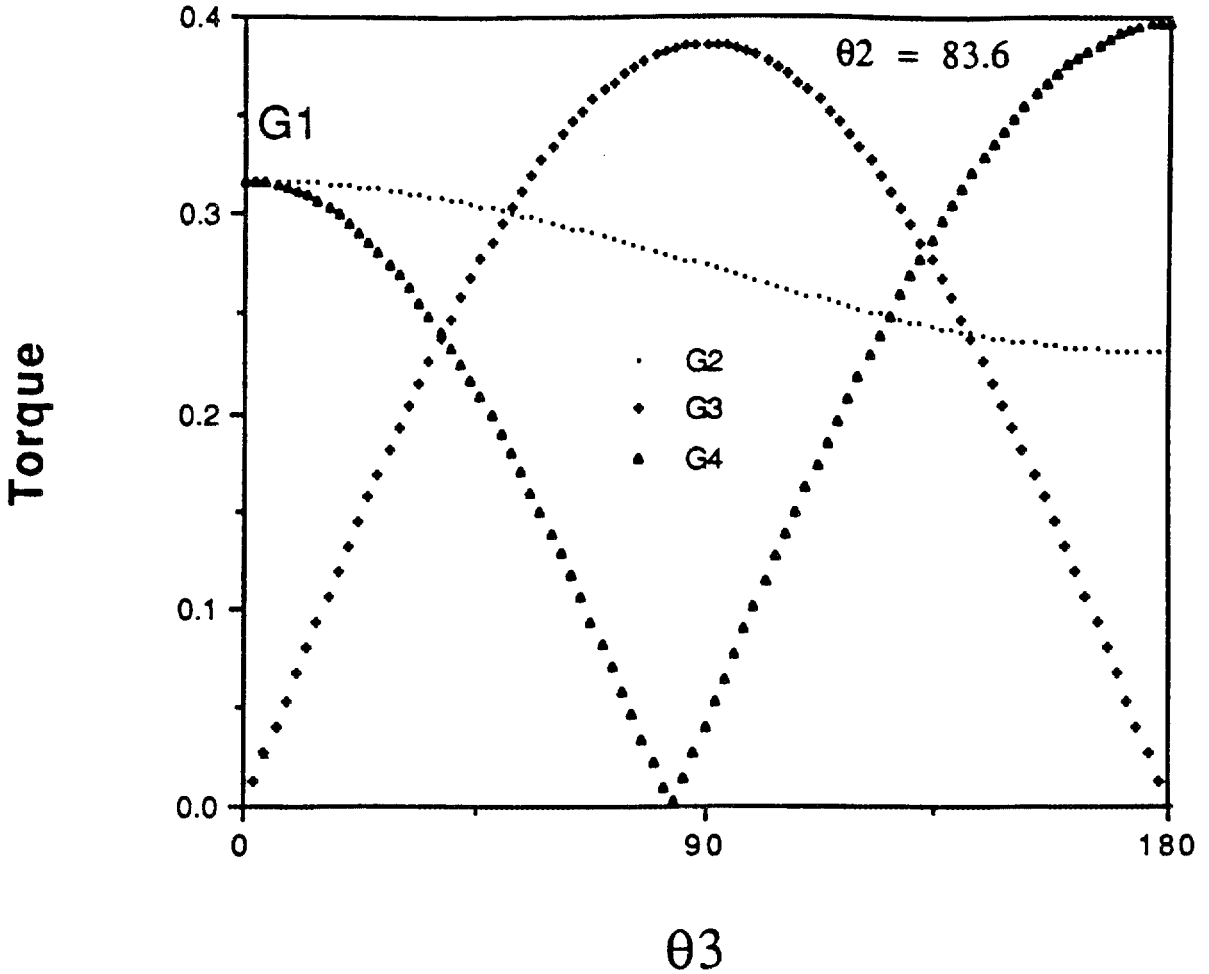

Fig. 19. Maximum torque (Q) versus angle (θ_3) when θ_2 = 83.6 and θ_4 = 45. The units of torque are newton meters and the units of angle are degrees.

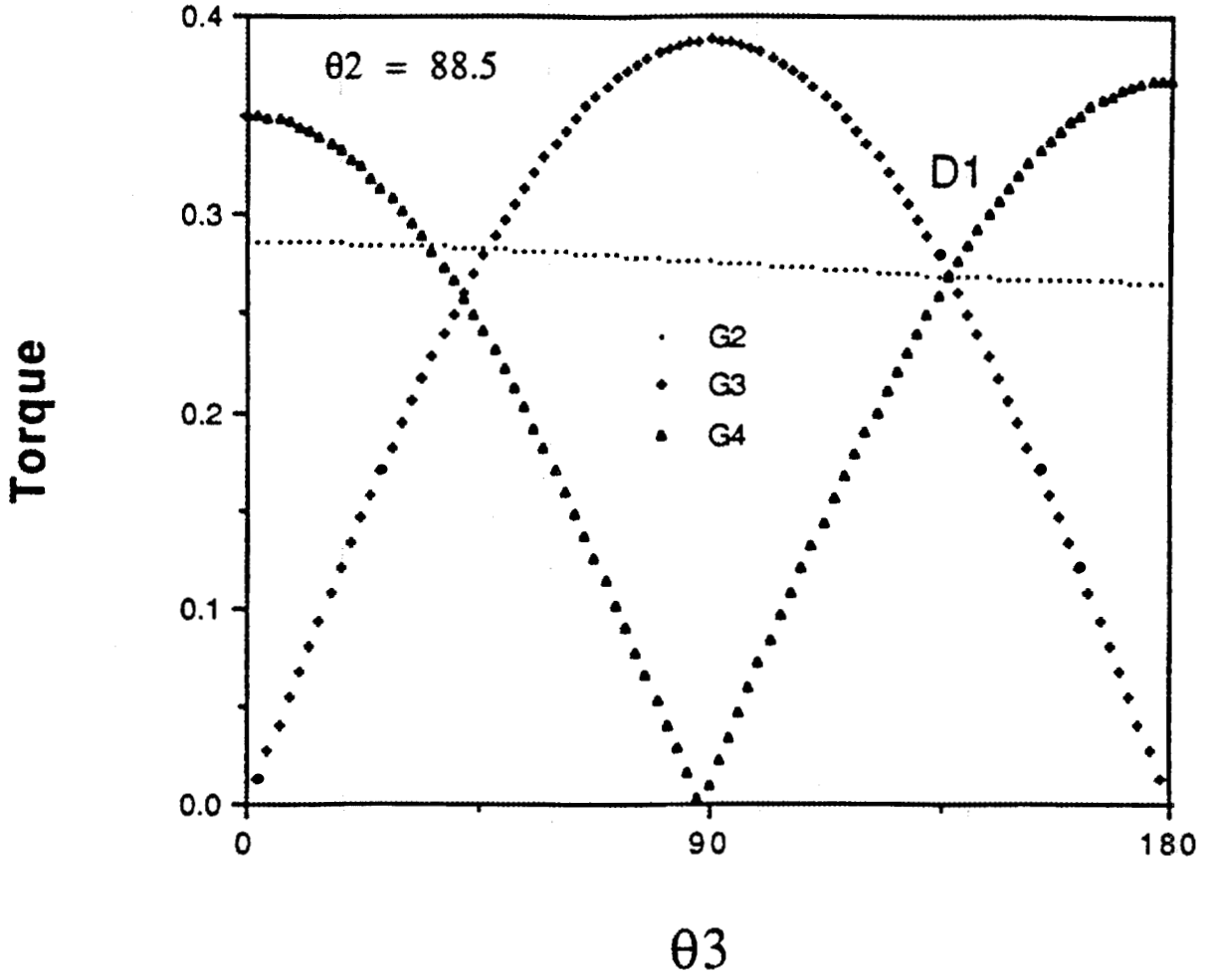

Fig. 20. Maximum torque (Q) versus angle (θ_3) when θ_2 = 88.5 and θ_4 = 45. The units of torque are newton meters and the units of angle are degrees.

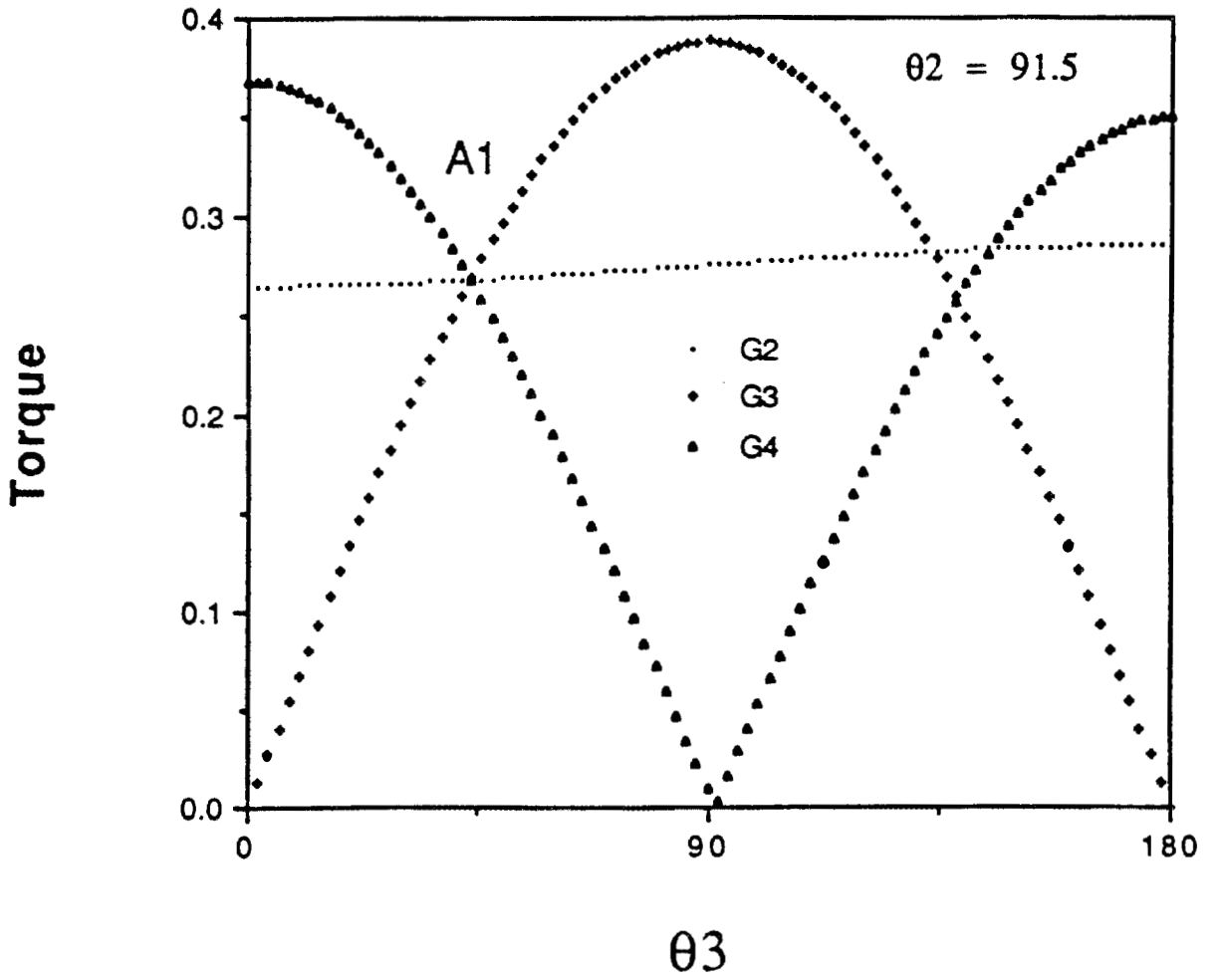

Fig. 21. Maximum torque (Q) versus angle (θ_3) when θ_2 = 91.5 and θ_4 = 45. The units of torque are newton meters and the units of angle are degrees .

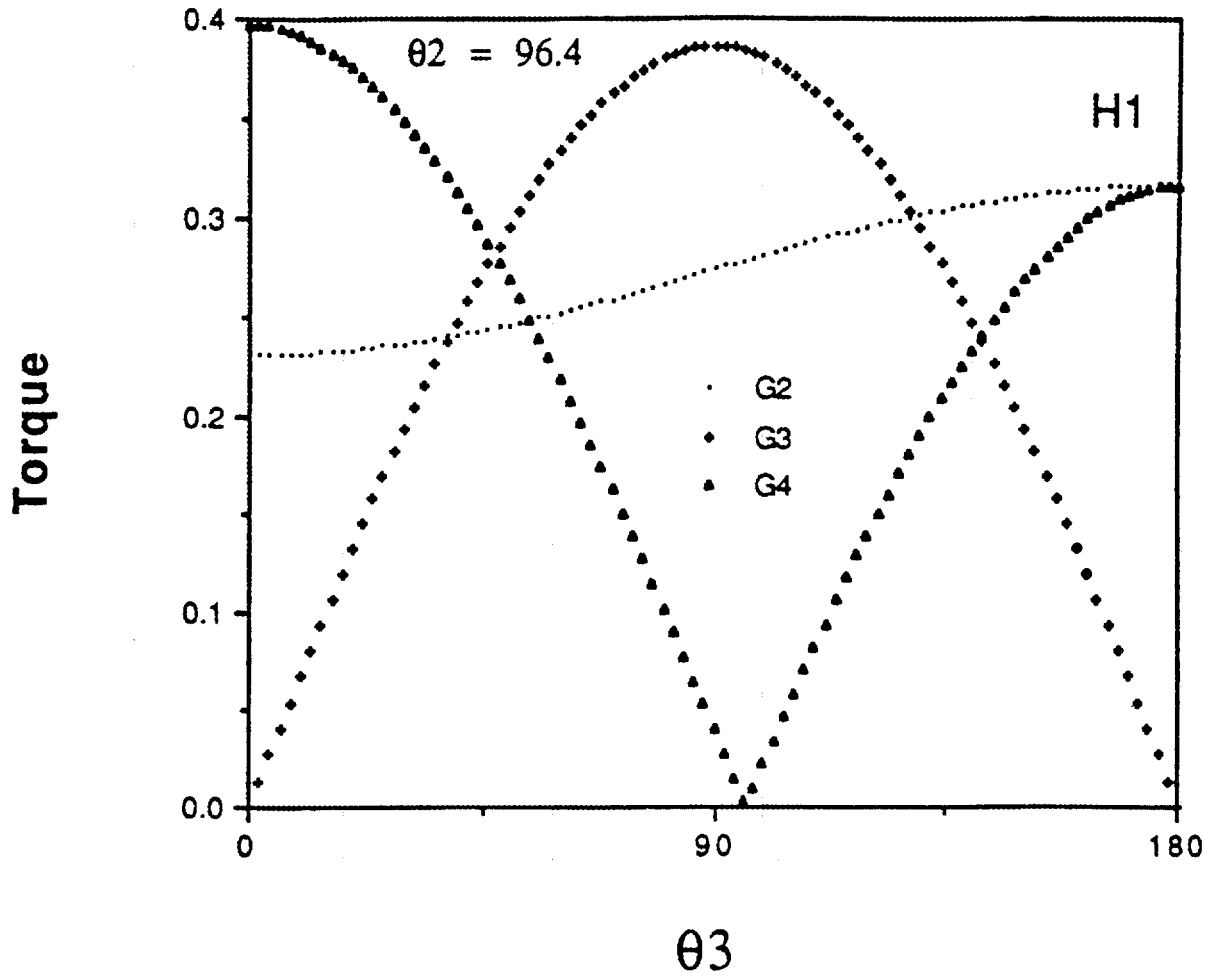

Fig. 22. Maximum torque (Q) versus angle (θ_3) when θ_2 = 96.4 and θ_4 = 45. The units of torque are newton meters and the units of angle are degrees.

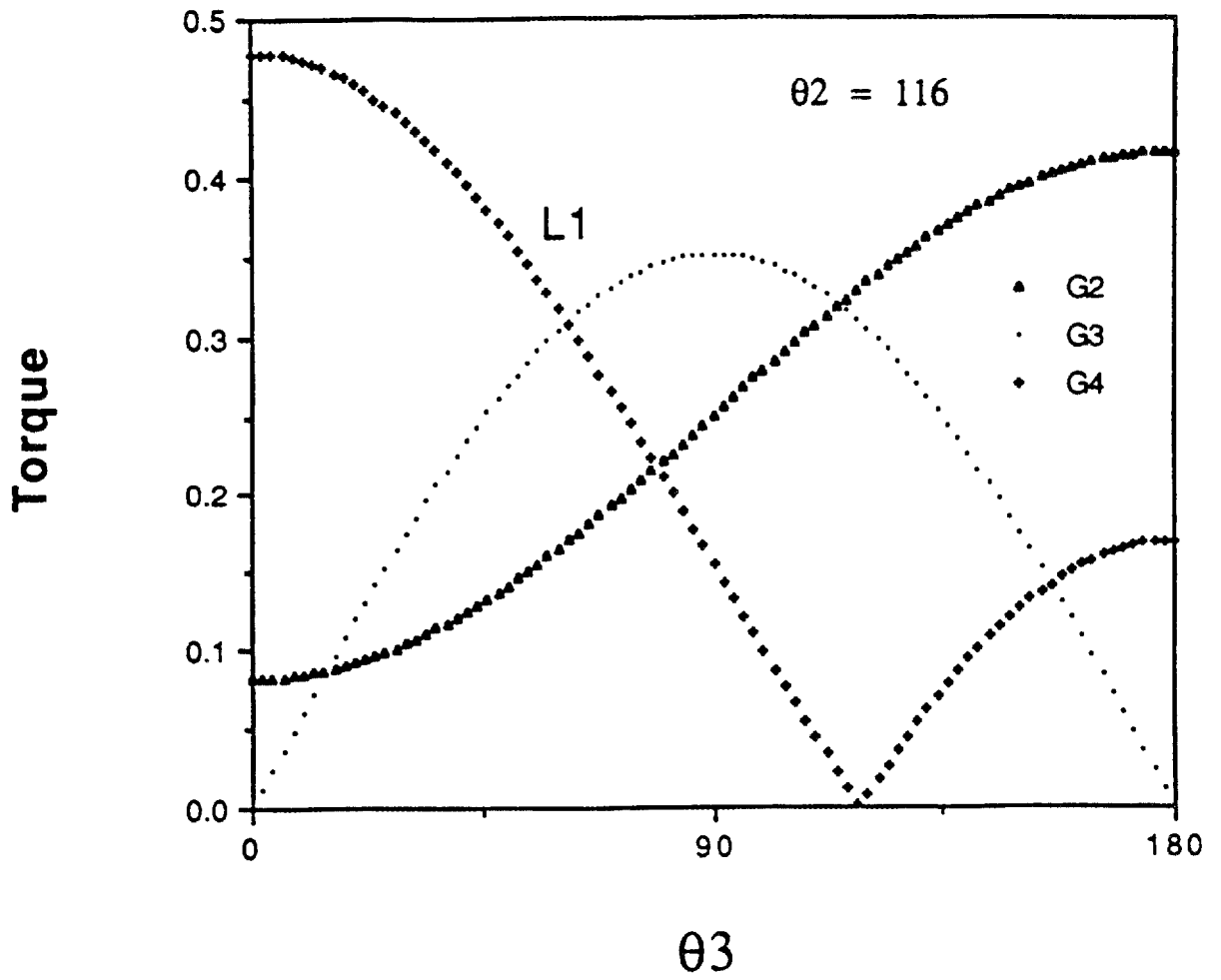

Fig. 23. Maximum torque (Q) versus angle (θ_3) when θ_2 = 116 and θ_4 = 45. The units of torque are newton meters and the units of angle are degrees.

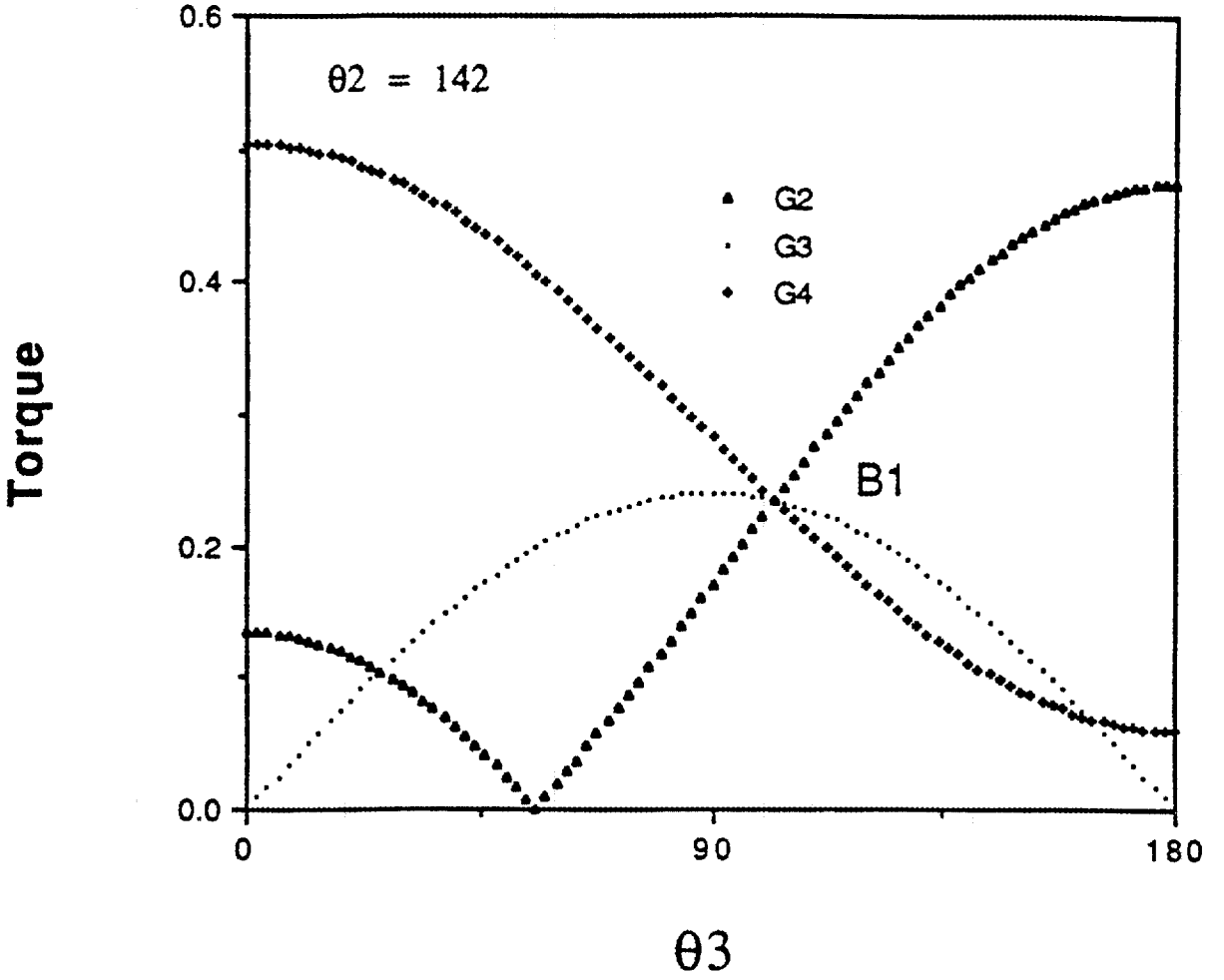

Fig. 24. Maximum torque (Q) versus angle (θ_3) when θ_2 = 142 and θ_4 = 45. The units of torque are newton meters and the units of angle are degrees.

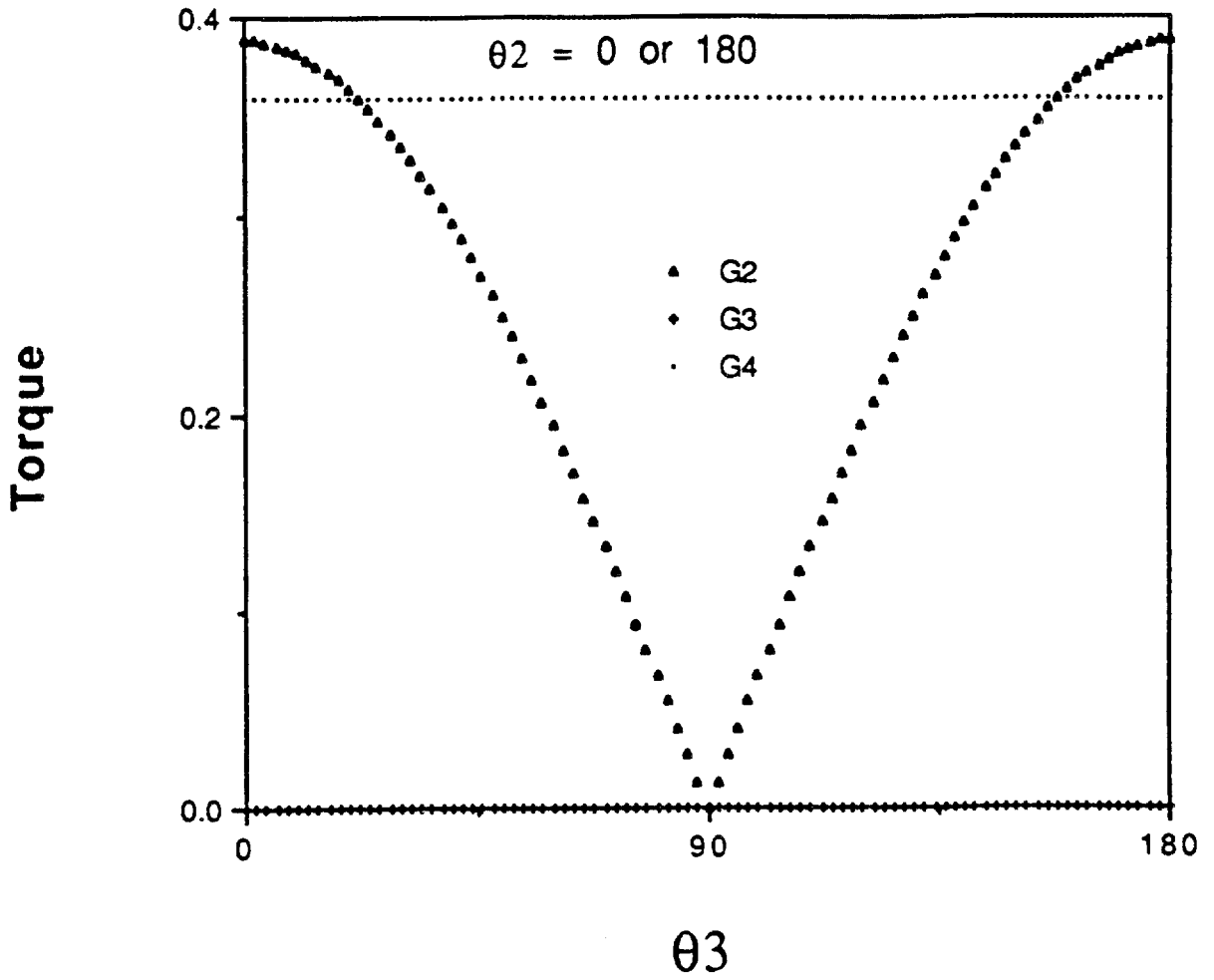

Fig. 25. Maximum torque (Q) versus angle (θ_3) when θ_2 = 180 and θ_4 = 45. The units of torque are newton meters and the units of angle are degrees.

The sequence of figures (Figs. 17 to 25) provides us with an opportunity to examine some of our assumptions. The figures display the surface of Q as a function of θ_2 and θ_3. In general, each local minima on the Q surface could be a Class 1, Class 2, or Class 3 point. In Figs. 17 and 25, there is a interval where Q is constant . For the initial and final points two torques are equal but for the interior values only one of the torques (G^4) is equal to Q. Although the derivative of G^4 with respect to θ_3 is zero in the interval, the derivative with respect to θ_2 is not zero except at the point where $\theta_3 = 90$ degrees. This point is not a local minimum, it is a saddle point (minimum with respect to θ_3 and maximum with respect to θ_2). In all of the other figures, the minimum values of Q occur when two or three torques are equal. Thus, there are no Class 1 points in the sequence of figures.

Figure14 is a network diagram that connects the significant points on the bridge paths with straight lines. We will now display the actual shape of the bridge paths. We begin with the equal bridge paths, the paths that connect the points A, B, C, and D. A closeup of the equal bridge paths is given in Fig. 26. Figure 27 displays both the equal paths (upper and lower) and the bridge paths. While there is a significant increase in torque in moving from A to D, the maximum values are less than the unoptimized values in Fig. 12.

The bridge for the long path begins at G, moves to A, and can take either of the two paths from A to D. A closeup of the long bridge path via point C is displayed in Fig. 28. Fig. 29 plots both segments of the long path and the bridge. The paths from G to A and from H to D are very close to straight lines.

By exploring paths where the magnitudes of two or three of the torques are equal during the motion, we have found three types of paths that are continuous in joint space: Equal, Long, and Bridge . Next, we will determine which paths satisfy the necessary conditions [Eqs.(14), (15) and (16)]. We begin by determining the elements of the A matrix [see Eq. (22)]. For the CESARm (and the planar manipulator), the functions $G^i(\theta)$ are given by:

$$G^i(\theta) = d_i\, J_i \tag{61}$$

where the constants $d_i = \pm 1$ and the signs are chosen to make the $G^i(\theta)$ nonnegative. We define the matrix $\Omega(\theta)$ by:

$$\Omega_{ij} = \frac{\partial J_i(\theta)}{\partial \theta_j} = \frac{\partial^2 f(\theta)}{\partial \theta_i \partial \theta_j} \tag{62}$$

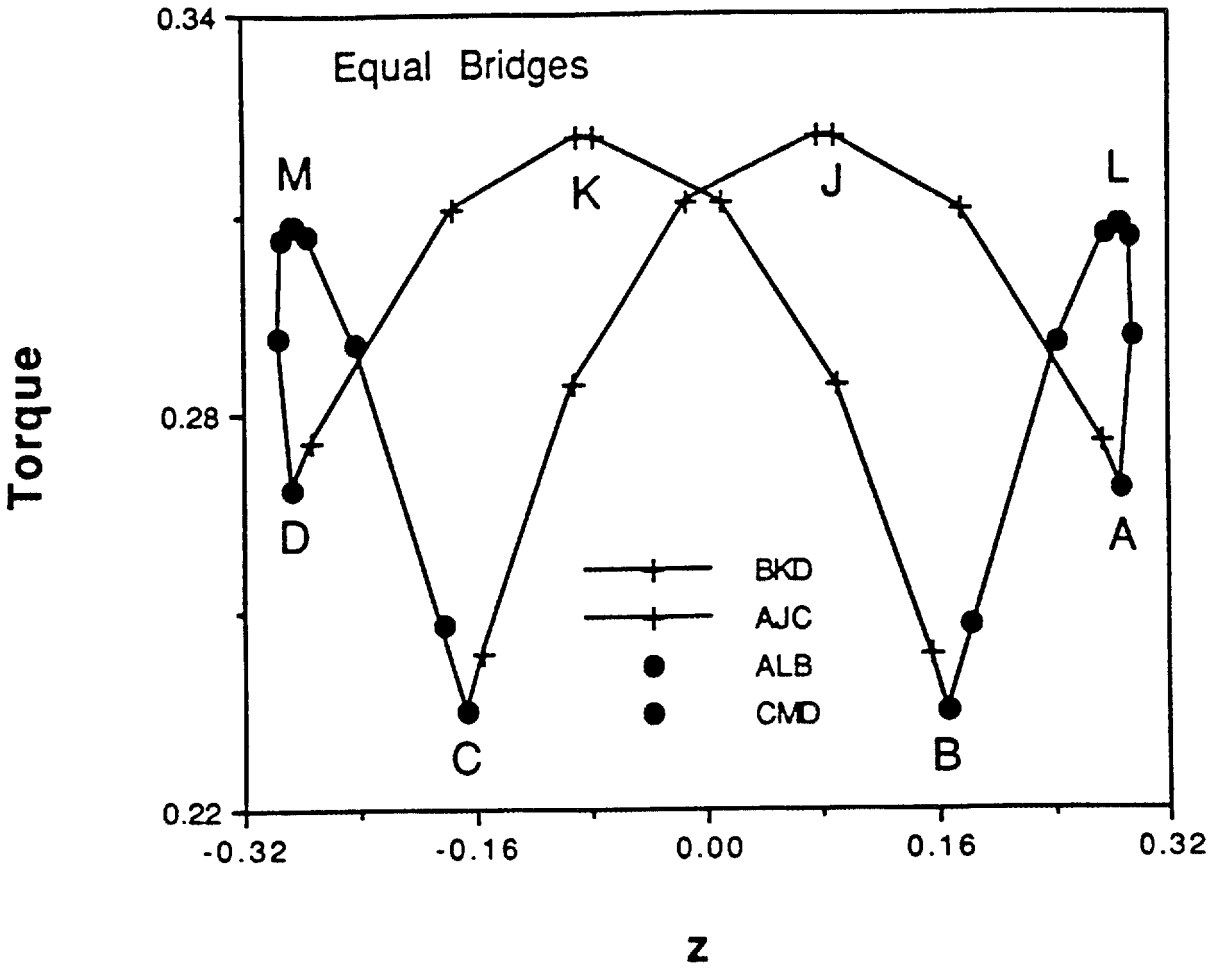

Fig. 26. A closeup of the Equal bridge paths. Maximum torque (Q) versus height (z). The units of torque are newton meters and the units of height are meters.

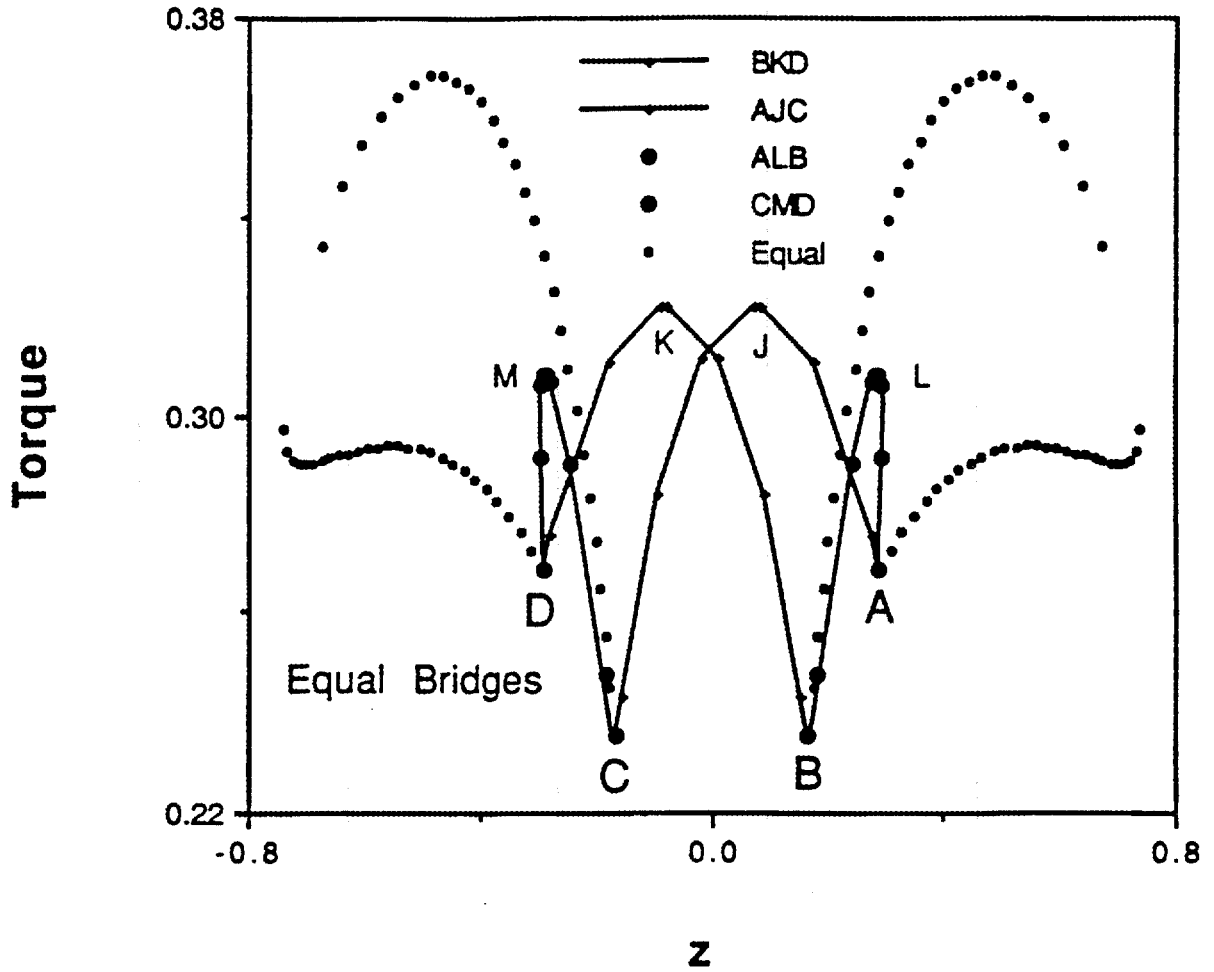

Fig. 27. The Equal paths and their bridge paths. Maximum torque (Q) versus height (z). The units of torque are newton meters and the units of height are meters.

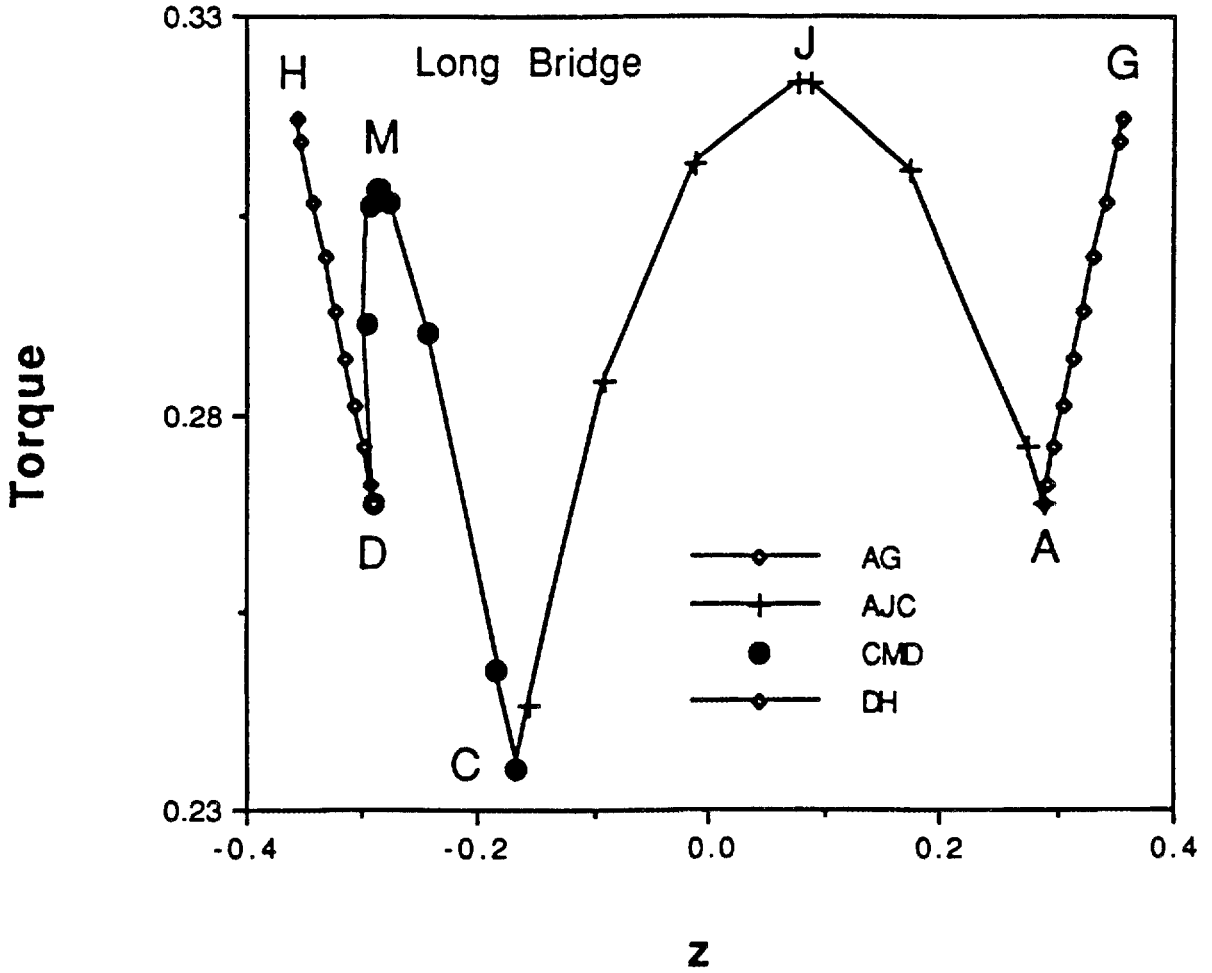

Fig. 28. A closeup of the Long bridge paths. Maximum torque (Q) versus height (z). The units of torque are newton meters and the units of height are meters.

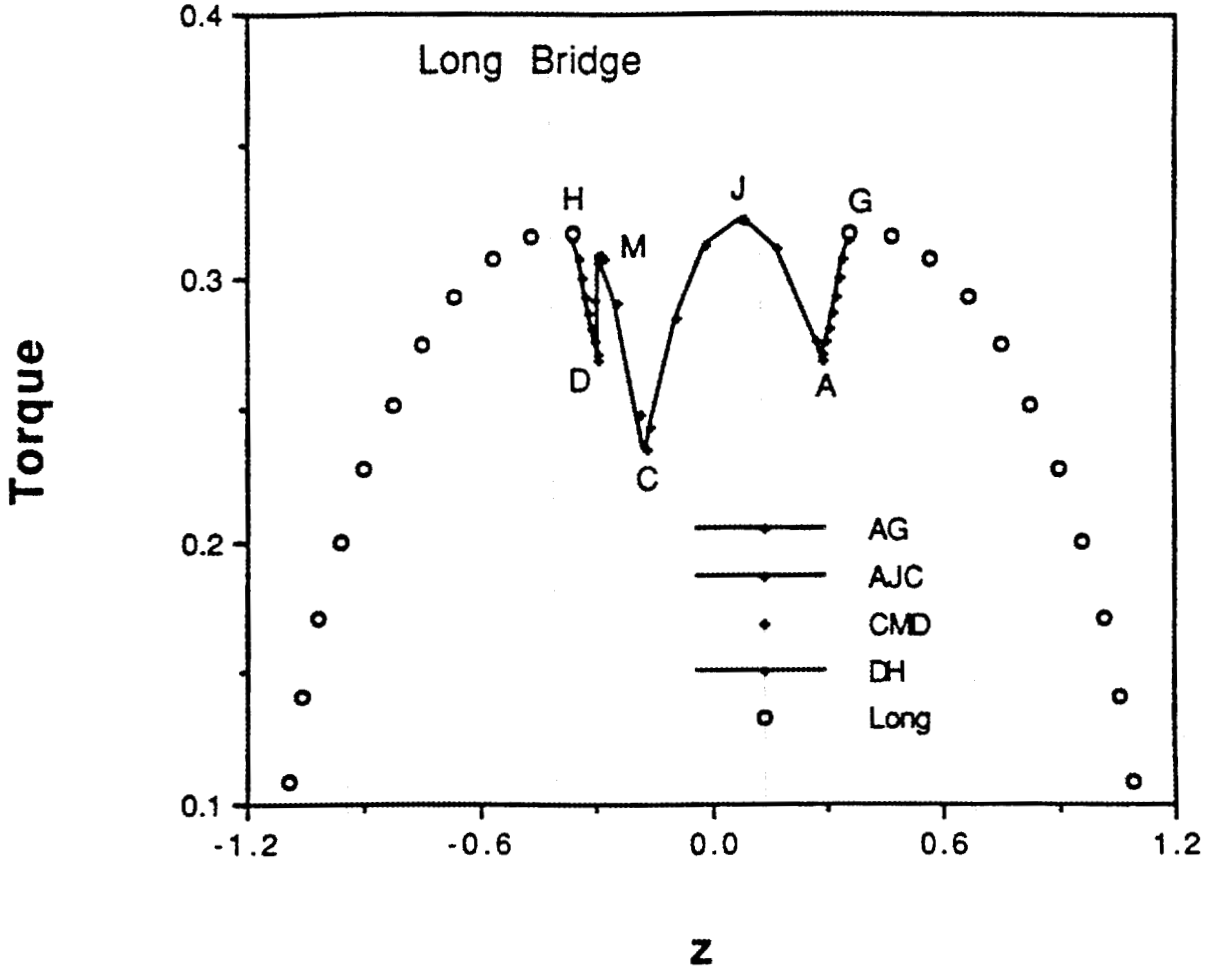

Fig. 29. The Long paths and their bridge paths. Maximum torque (Q) versus height (z). The units of torque are newton meters and the units of height are meters.

The matrix Ω will be symmetric:

$$\Omega_{22} = - s_2 c_3 D - c_2 H \tag{63}$$

$$\Omega_{23} = - c_2 s_3 D \tag{64}$$

$$\Omega_{24} = - a_4 s_2 c_4 - a_4 c_2 c_3 s_4 \tag{65}$$

$$\Omega_{33} = - s_2 c_3 D \tag{66}$$

$$\Omega_{34} = a_4 s_2 s_3 s_4 \tag{67}$$

$$\Omega_{44} = - a_4 s_2 c_3 c_4 - a_4 c_2 s_4 \tag{68}$$

Using the matrix Ω, the A matrix is:

$$A^T = \begin{bmatrix} d_2 \Omega_{22} & d_3 \Omega_{23} & d_4 \Omega_{24} \\ d_2 \Omega_{32} & d_3 \Omega_{33} & d_4 \Omega_{34} \\ d_2 \Omega_{42} & d_3 \Omega_{43} & d_4 \Omega_{44} \end{bmatrix} \tag{69}$$

Our goal is to find the μ_i that satisfy the first order necessary conditions [Eqs. (14) to (16)]. We will introduce the intermediate vector ($\eta_i = \mu_i / \lambda$) and solve Eq. (15) to find the values of η_i. We can choose the normalization factor (λ) to insure that Eq. (14) is satisfied:

$$\lambda = 1 / \sum_i \eta_i \tag{70}$$

$$\mu_i = \lambda * \eta_i \tag{71}$$

The remaining condition is that the μ_i must not be negative [Eq. (16)]. Thus, the μ_i satisfy the necessary conditions if the η_i all have the same sign.

Table 8 provides a summary of our evaluation of the necessary conditions for the lower branch of the Equal path. The first six points do not satisfy the necessary conditions while the last six points do satisfy the conditions. In Fig. 13, the initial section of the lower branch of the Equal path is higher than the Long path. All points on the Long path satisfy the necessary conditions (see Table 9).

For the Bridge paths, θ_4 is constant and we will evaluate the necessary conditions for both a function of all three joint variables and a function of the first two variables. We present the results for the Bridge path from A to B in Table 10. The results for the path from C to D are the same as the results in Table 10. Considering all three joint variables, the Bridge path satisfies the necessary conditions for the first four points and fails the test for the last two points. Thus, the Class 3 points B and C (the lowest points in Fig. 14) do not satisfy the necessary conditions. Considering the first two joint variables, the Bridge path satisfies the necessary conditions for the first three points and the last point while failing the test for two intermediate points.

Table. 8. Evaluation of the necessary conditions for the lower branch of the Equal path.

n	θ_4	z	Q	Satisfy?
1	-10	0.74	0.30	No
2	-5	0.72	0.29	No
3	0	0.69	0.29	No
4	5	0.66	0.29	No
5	10	0.61	0.29	No
6	15	0.58	0.29	No
7	20	0.53	0.29	Yes
8	25	0.49	0.29	Yes
9	30	0.43	0.29	Yes
10	35	0.39	0.29	Yes
11	40	0.34	0.28	Yes
12	45	0.29	0.27	Yes

Table 9. Evaluation of the necessary conditions for the Long path.

n	θ_4	z	Q	Satisfy?
1	-55	1.09	0.11	Yes
2	-30	0.99	0.19	Yes
3	-5	0.82	0.25	Yes
4	20	0.62	0.30	Yes
5	45	0.36	0.32	Yes

Table 10. Evaluation of the necessary conditions for the Bridge path from A to B.

				Satisfy?	
n	θ_2	z	Q	3X3	2X2
1	91	0.29	0.27	Yes	Yes
2	100	0.30	0.29	Yes	Yes
3	110	0.29	0.31	Yes	Yes
4	120	0.28	0.31	Yes	No
5	130	0.24	0.29	No	No
6	142	0.17	0.24	No	Yes

For the Bridge path from A to C (see Table 11), the path satisfies the 3X3 necessary conditions for the first three points and fails the test for the last three points. The path satisfies the 2X2 necessary conditions at all points. The results for the path from B to D are the same as the results in Table 11.

Table 11. Evaluation of the necessary conditions for the Bridge path from A to C.

				Satisfy?	
n	θ_2	z	Q	3X3	2X2
1	91	0.29	0.27	Yes	Yes
2	80	0.17	0.31	Yes	Yes
3	70	0.08	0.32	Yes	Yes
4	60	-0.01	0.31	No	Yes
5	50	-0.09	0.28	No	Yes
6	38	-0.17	0.24	No	Yes

The results for the Bridge path from A to G (and D to H) are summarized in Table 12. The path satisfies both the 3X3 necessary conditions and the 2X2 necessary conditions at all points. The path from B to E is evaluated in Table 13. The path does not satisfy the 3X3 necessary conditions at any point except the last point. The path satisfies the 2X2 necessary conditions at all points.

Finally, we shall consider the Class 1 paths. For Class 1, one of the $G^i(\theta)$ is larger than the others and it must satisfy the conditions of classical optimization [Eq. (19)]. The

elements of the A matrix are the partial derivatives of the $G^i(\theta)$. If G^2 is largest, the classical optimization conditions require that the first column of the A^T matrix will be zero. If G^3 is largest, the second column of the A^T matrix will be zero and if G^4 is largest, the third column will be zero.

If the first column of the A^T matrix is zero, then Ω_{23} will be zero:

$$c_2 \, s_3 \, D = 0 \tag{72}$$

D cannot be zero. (If $D = 0$, $\theta_4 = \pm 93$ degrees. The allowable range for θ_4 is from -55 degrees to 45 degrees.) If Ω_{23} is zero, then either $c_2 = 0$ or $s_3 = 0$.

Table 12. Evaluation of the necessary conditions for the Bridge path from A to G.

				Satisfy?	
n	θ_2	**z**	**Q**	**3X3**	**2X2**
1	91	0.29	0.27	Yes	Yes
2	90	0.30	0.28	Yes	Yes
3	89	0.31	0.28	Yes	Yes
4	88	0.31	0.29	Yes	Yes
5	87	0.32	0.29	Yes	Yes
6	86	0.33	0.30	Yes	Yes
7	85	0.34	0.31	Yes	Yes
8	84	0.36	0.32	Yes	Yes

Table 13. Evaluation of the necessary conditions for the Bridge path from B to E.

				Satisfy?	
n	θ_2	**z**	**Q**	**3X3**	**2X2**
1	142	0.17	0.24	No	Yes
2	150	0.17	0.25	No	Yes
3	160	0.19	0.28	No	Yes
4	170	0.22	0.31	No	Yes
5	180	0.28	0.36	Yes	Yes

For the first case, if $c_2 = 0$ and $\Omega_{22} = 0$ then $c_3 D = 0$. Since D cannot be zero, $c_3 = 0$. If $c_2 = 0$, $c_3 = 0$, and $\Omega_{24} = 0$, then $c_4 = 0$. However, the points where $c_4 = 0$ are outside the allowable range for θ_4. Thus, there is not a Class 1 solution for this case.

For the other set of Class 1 solutions, $s_3 = 0$. If Ω_{24} is zero:

$$T_2 = -c_3 T_4 \tag{73}$$

Given θ_4, Eq. (73) can be used to determine θ_2. For example, if $\theta_3 = 0$ then $\theta_2 = -\theta_4$ or $\theta_2 = \pi - \theta_4$. There are four sets of solutions (two values of θ_2 when $\theta_3 = 0$ and two values of θ_2 when $\theta_3 = \pi$). For all four sets of solutions, $G^4 = a_4 = 0.508$ newton meters. Thus, the minimum value of $Q(\theta)$ cannot be less than 0.508. Hence, these four Class 1 solutions have much higher values for $Q(\theta)$ than the best Class 2 and Class 3 paths (see Figs. 27 and 29).

If the second column of the A^T matrix is zero, then Q_{23} will be zero and either $c_2 = 0$ or $s_3 = 0$. For the first case, if $c_2 = 0$ and $\Omega_{33} = 0$ then $c_3 = 0$. If $c_2 = 0$, $c_3 = 0$, and $\Omega_{34} = 0$, then $s_4 = 0$. At these points: $G^2 = 0.635$, $G^3 = 0.537$, and $G^4 = 0$. Thus, $Q(\theta) = 0.635$ newton meters and G^3 is not the largest value. Thus, there is not a Class 1 solution for this case.

For the second case, if $s_3 = 0$ and $\Omega_{33} = 0$ then $s_2 = 0$ and $\Omega_{34} = 0$. If $s_3 = 0$ and $s_2 = 0$, $G^2 = D$, $G^3 = 0$, and $G^4 = D - a_3$. Thus, $Q(\theta) = D$ and G^3 is not the largest value. Thus, there is not a Class 1 solution for this case.

The third column of the A^T matrix will be zero if $s_2 = 0$ and $s_4 = 0$. For this case: $G^2 = c_3 D$, $G^3 = 0$, and $G^4 = 0.508$. If the magnitude of θ_3 is greater than 18.9 degrees, G^4 will be the largest of the G^i and $Q(\theta) = 0.508$ newton meters. Thus, this case has a Class 1 solution.

The second case for which the third column of the A^T matrix will be zero is when $s_3 = 0$ and Eq. (73) is satisfied. This is the same as the second case when the first column of the A^T matrix was zero.

We have examined all of the possible Class 1 solutions. In all cases, the minimum value of $Q(\theta)$ cannot be less than 0.508 newton meters. Hence, all Class 1 solutions have much higher values for $Q(\theta)$ than the best Class 2 and Class 3 paths (see Figs. 27 and 29).

5. CONCLUSIONS

We have considered the problem of determining the time trajectories of the joint variables of a mobile manipulator with many redundant degrees of freedom that will minimize the maximum value of the torque during a large scale motion by the manipulator. To create a well defined problem, we have divided the problem into two components: path planner and surveyor. The path planner chooses a path between two points in Cartesian space that will minimize the maximum value of the torque along the path. The input to the path planner is a network of path segments with the maximum value of the torque on each segment. The surveyor explores the joint space, calculates the Cartesian position and maximum torque, and defines the network of path segments. In this paper, our focus has been on the surveyor and not on the path planner.

There is a large literature on algorithms for the solution of min-max problems. However, our min-max problem has an extra constraint on the joint variables. We have used the Kuhn-Tucker conditions to derive necessary conditions for the solution of our min-max problem. We find that the necessary conditions require that at one or more of the joints the magnitude of the normalized torques will be equal to the min-max value. We have classified the sets of points that satisfy the necessary conditions based on the number of the normalized torques t hat are equal to the min-max value. We have solved the min-max problem by identifying all of the points in all of the classes.

Our surveyor is experienced and uses a rule of thumb: follow valleys. Valleys are the intersections of two or more of the joint torque surfaces $[G^i(\theta)]$. Along the valleys, the magnitudes of two or more of the joint torques will be equal. Valleys are good locations for low torque paths. The surveyor has explored two examples: a planar manipulator and the CESARm.

The mobile planar manipulator has three revolute joints. We began by exploring the Class 3 paths. We defined four cases and 16 subcases. For each of the 16 subcases, we have defined the three link angles in terms of a single parameter. By relating the three link angles to the parameter, we have resolved the redundancy.

We have found that 13 of the 16 subcases satisfy the necessary conditions. Of the 13 subcases, there are five configurations with a one meter workspace, three configurations with a three meter workspace, and one configuration with a five meter workspace. Given an initial value for z and a final value, the path planner will choose one of the 13 options. All but one of the options has a portion of the workspace where it is superior to any of the other options. Thus, the Class 3 paths reach all parts of the workspace.

We have explored Class 2 and Class 1 paths. We have surveyed Class 2 paths for a constant value of z. By examining Class 2 paths, we have been able to identify all 10 of the Class 3 subcases that can reach the point z = 0.25. In 8 of the 10 subcases, we have found a local minima. All of the local minima for the Class 2 paths occurred at points where the torques were equal at all three joints. Thus, we were unable to find any Class 2 local minima. All of the Class 1 solutions had higher values for the torque than the best Class 3 paths.

The CESARm is a manipulator with 7 degrees of freedom that can reach points in 3D space. We assumed that the CESARm is mounted on a mobile platform that will control the x and y coordinate of the arm's tip We have three joint angles controlling the height of the arm (z). We explored the Class 3 paths. There are four ways that three torques can be equal. For the planar manipulator, the four cases were distinct. For the CESARm, the four cases correspond to changes of variables. We found four segments for the Class 3 paths. While the four segments have low values for the maximum torque, they only cover part of the workspace and do not join together.

By exploring Class 2 paths, we have found paths that cover the workspace and bridge between the disjoint Class 3 path segments. We have evaluated the necessary conditions for both the Class 3 paths and the Class 2 paths. In most cases, the paths satisfy the necessary conditions.

We have examined all of the possible Class 1 solutions. In all cases, the minimum value of the torque cannot be less than 0.508 newton meters. Hence, all Class 1 solutions have much higher values for the torque than the best Class 2 and Class 3 paths.

REFERENCES

1. Pin, F. G. and J. C. Culioli, "Optimal Positioning of Combined Mobile Platform Manipulator Systems for Material Handling Tasks," *Journal of Intelligent and Robotic Systems*, **6**, 165-182 (1992).

2. Pin, F. G. and J. C. Culioli, "Optimal Positioning of Redundant Manipulator-Platform Systems for Maximum Task Efficiency," *Robotics and Manufacturing*, **3**, 489-495 (1990).

3. Pin, F. G. J. C. Culioli and D. B. Reister, "Using Minimax Approaches to Plan Optimal Task Commutation Configurations for Combined Mobile Platform-Manipulator Systems," *IEEE Transactions on Robotics and Automation* (in press).

4. Polak, E., D. Q. Mayne, and J. E. Higgins, "Superlinearly Convergent Algorithm for Min-Max Problems," *Journal of Optimization Theory and Applications*, 69, 407-439 (1991).

5. Dubey, R. V., J. A. Euler, and S. M. Babcock, "Real-Time Implementation of an Optimization Scheme for Seven-Degree-of-Freedom Redundant Manipulators," *IEEE Transactions on Robotics and Automation*, 579-588 (1991).

6. Press, W. H. et al. 1988. *Numerical Recipes in C: The Art of Scientific Computing*. Cambridge, UK: Cambridge University Press.

APPENDIX

FORMULAS FOR TWO EQUAL TORQUES

With θ_4 constant, we vary θ_2 from -180 degrees to 180 degrees. For each value of θ_2, we find all of the values for θ_3 that have equal magnitudes for two of the three torques. For each value of θ_2, there can be as many as six values for θ_3 ($J_2 = \pm J_3$, $J_2 = \pm J_4$, and $J_3 = \pm J_4$.). In this appendix, we will derive formulas for the six expressions for θ_3.

Assume that $J_2 = K J_3$ (where $K = \pm 1.0$). Then:

$$c_2 c_3 D - s_2 H = - K s_2 s_3 D \tag{A1}$$

Gathering the terms involving θ_3 on the left:

$$(c_2 c_3 + K s_2 s_3) D = s_2 H \tag{A2}$$

Using the addition formula for cosine:

$$\cos(\theta_3 - K \theta_2) = s_2 H / D \tag{A3}$$

If $|s_2 H / D| < 1.0$, define δ by:

$$\cos(\delta) = s_2 H / D \tag{A4}$$

Then the solution of Eq. (A3) is:

$$\theta_3 = K \theta_2 + \delta \tag{A5}$$

Assume that $J_2 = K J_4$. Then:

$$c_2 c_3 D - s_2 H = - K a_4 s_2 c_3 s_4 + K a_4 c_2 c_4 \tag{A6}$$

Gathering the terms involving θ_3 on the left:

$$c_3 (c_2 D + K a_4 s_2 s_4) = s_2 H + K a_4 c_2 c_4 \tag{A7}$$

Eq. (A7) may be written:

$$\cos(\theta_3) = (s_2 H + K a_4 c_2 c_4) / (c_2 D + K a_4 s_2 s_4) \tag{A8}$$

Assume that $J_3 = K J_4$. Then:

$$- s_2 s_3 D = - K a_4 s_2 c_3 s_4 + K a_4 c_2 c_4 \tag{A9}$$

Gathering the terms involving θ_3 on the left:

$$c_3 (K a_4 s_2 s_4) - s_3 (s_2 D) = K a_4 c_2 c_4 \tag{A10}$$

Define δ and ρ by:

$$\rho \cos \delta = K a_4 s_2 s_4 \tag{A11}$$

$$\rho \sin \delta = s_2 D \tag{A12}$$

Eq. (A10) may be written:

$$\rho (c_3 \cos \delta - s_3 \sin \delta) = K a_4 c_2 c_4 \tag{A13}$$

Using the addition formula for cosine:

$$\cos(\theta_3 - \delta) = K a_4 c_2 c_4 / \rho \tag{A14}$$

If $|a_4 c_2 c_4 / \rho| < 1.0$, define ε by:

$$\cos(\varepsilon) = K a_4 c_2 c_4 / \rho \tag{A15}$$

Then the solution of Eq. (A14) is:

$$\theta_3 = \delta + \varepsilon \tag{A16}$$

INTERNAL DISTRIBUTION

1. B. R. Appleton
2. J. E. Baker
3. M. Beckerman
4. C. W. Glover
5. J. P. Jones
6. H. E. Knee
7-11. R. C. Mann
12. E. M. Oblow
13-17. F. G Pin
18. V. Protopopescu
19-23. D. B. Reister
24. E. C. Uberbacher
25. M. A. Unseren
26-30. R. C. Ward
31. EPMD Reports Office
32-33. Laboratory Records Department
34. Laboratory Records, ORNL-RC
35. Document Reference Section
36. Central Research Library
37. ORNL Patent Section

EXTERNAL DISTRIBUTION

38. Dr. Peter Allen, Department of Computer Science, 450 Computer Science, Columbia University, New York, NY 10027
39. Dr. John Baillieul, Aerospace and Mechanical Engineering Department, Boston University, 110 Cummington St., Boston, MA 02215
40. Dr. Wayne Book, Department of Mechanical Engineering, J. S. Coon Building, Room 306, Georgia Institute of Technology, Atlanta, GA 30332
41. Professor Roger W. Brockett, Harvard University, Pierce Hall, 29 Oxford St., Cambridge, MA 02138
42. Dr. Steven Dubowsky, Massachusetts Institute of Technology, Building 3, Room 469A, 77 Massachusetts Ave., Cambridge, MA 02139
43. Professor Donald J. Dudziak, Dept. of Nuclear Engineering, 110B Burlington Engineering Labs, North Carolina State University, Raleigh, NC 27695-7909
44. Mr. Steve Holland, Robotics, B/MD-63, General Motors Corporation, NAO Manufacturing Center, 30300 Mound Rd., Warren, MI 48090-9040
45. Dr. Avi Kak, Department of Electical Engineering, Purdue University, Northwestern Ave., Engineering Mall, Lafayette, IN 47907
46. Professor Takeo Kanade, Computer Science and Robotics, Carnegie Mellon University, Pittsburgh, PA 15213-3890
47. Dr. James E. Leiss, Route 2, Box 142C, Broadway, VA 22815
48. Dr. Oscar P. Manley, Division of Engineering, Mathematical, and Geosciences, Office of Basic Energy Sciences, ER-15, U.S. Department of Energy - Germantown, Washington, DC 20545
49. Professor Neville Moray, Department of Mechanical and Industrial Engineering, University of Illinois, 1206 West Green St., Urbana, IL 61801
50. Dr. Wes Snyder, Department of Radiology, Bowman Gray School of Medicine, 300 S. Hawthorne Dr., Winston-Salem, NC 27103
51. Professor Mary F. Wheeler, Department of Mathematical Sciences, Rice University, P.O. Box 1892, Houston, TX 77251
52. Office of Assistant Manager for Energy Research and Development, U.S. Department of Energy, Oak Ridge Operations Office, P.O. Box 2001, Oak Ridge, TN 37831-8600

53-54. Office of Scientific and Technical Information, P.O. Box 62, Oak Ridge, TN 37831